

0.35 μm CMOS C35 RF SPICE Models

Seven Digit Document: ENG-188

Revision #: 5.0

Table of Contents

1	Introduction.....	3
1.1	Revision.....	3
1.2	Process Family.....	3
1.3	Related Documents	3
2	MOS Transistor RF Models (modnrf and modprf)	4
2.1	Cross-Section and Device Definition.....	4
2.2	Subcircuit Model.....	5
2.3	Main Parameters	5
2.4	Characteristic Curves	5
3	MOS Varactor Model (cvar).....	10
3.1	Cross-Section, Layout and Device Definition.....	10
3.2	Subcircuit Model.....	11
3.3	Main Parameters	12
3.4	Characteristic Curves	13
4	Inductor Models (STxxxAyyyB)	15
4.1	Subcircuit Model.....	15
4.2	Main Parameters	16
4.3	Characteristic Curves	18
5	Differential Inductor Models (DlxxPT)	24
5.1	Subcircuit Model.....	24
5.2	Main Parameters	25
5.3	Characteristic Curves	25
6	Poly1-Poly2 Capacitor (CPOLYRF)	29
6.1	Subcircuit Model.....	29
6.2	Main Parameters	29
6.3	Characteristic Curves	30
7	Metal-Metal Capacitor (CMIM).....	32
7.1	Subcircuit Model.....	32
7.2	Characteristic Curves	32
8	Poly Resistors (RPOLY2RF, RPOLYHRF).....	34
8.1	Subcircuit Model.....	34
8.2	Main Parameters	34
8.3	Characteristic Curves	35
9	Summary of RF SPICE Models.....	37
10	Simulator Models and Design Kit Integration.....	37
11	Note on S-parameter measurements	38
12	Support	38
13	Copyright	38

1 Introduction

The aim of this document is to provide designers with RF modeling and performance related information such as frequency and geometrical restrictions on validity of the models and subcircuits used to describe the behavior at RF. All RF characterized devices have been included. The RF SPICE Models document supplements the information found in the Process Parameters and Design Rules documents of the process.

1.1 Revision

Rev. 1.0	Affected pages: 1 to 22	October 2002
Subject of change: first version of RF SPICE Models		
Rev. 2.0	Affected pages: 12 to 20, 26	April 2003
Added: 4 metal and thick metal inductor models, Metal-Metal capacitor RF performance		
Rev. 3.0	Affected pages: 4 to 10	August 2003
Added: PMOS RF model and NMOS fmax plots		
Rev. 4.0	Affected pages: 1 to 33	May 2005
Revised: CVAR, CPOLYRF, RPOLY2RF (Narrower validity range for W=2 - 3 μm . Existing designs should be checked) Added: CMIMRF, RPOLYHRF, cross-sections of NMOSRF and PMOSRF		
Rev. 5.0	Affected pages: 1 to 38	October 2005
Added: Differential Inductors		

1.2 Process Family

This document is valid for the following 0.35 μm CMOS Processes:

Process name	No. of masks	CMOS core module *	POLY1-POLY2 capacitor module **	5 Volt module	High resistive poly module	Metal 4 module	Thick Metal module	MET2-METC capacitor module	Low VT module
C35A3B0	13	x							
C35B3C0	14	x	x						
C35B3C1	17	x	x	x					
C35B3C3	18	x	x	x	x				
C35B4C0	16	x	x			x			
C35B4C3	20	x	x	x	x	x			
C35B4M3	21	x	x	x	x		x	x	
C35B4M6	18	x	x		x	x		x	
C35B3L3	22	x	x	x	x				x

*) CMOS core module

consists of p-substrate, single poly, triple metal and 3.3 Volt process.

**) POLY1-POLY2 capacitor module

consists of p-substrate, double poly (RPOLY2 resistor), triple metal and 3.3 Volt process.

1.3 Related Documents

Description	Document Number
0.35 μm CMOS C35 Process Parameters	Eng-182
0.35 μm CMOS C35 Design Rules	Eng-183
0.35 μm CMOS C35 Noise Parameters	Eng-189
0.35 μm CMOS C35 Matching Parameters	Eng-228

2 MOS Transistor RF Models (modnrf and modprf)

Minimum length MOS transistors have been characterized at RF. Multi finger transistors are modeled as single transistors. The model is based on the BSIM3v3.1 model, where the internal D/B and S/B diodes are replaced by external diodes enabling substrate network modeling. The subcircuit extension of the BSIM3v3 model contains parasitic gate and substrate resistors along with external source and drain resistors. The model scales with the number of gate fingers connected in parallel.

The model is valid in the following range:

Frequency range: up to 6 GHz

Maximum width: NMOS: 200 μm , PMOS: 150 μm

Width of a single finger: 5 or 10 μm

Gate fingers contacted on one side

Length: 0.35 μm

2.1 Cross-Section and Device Definition

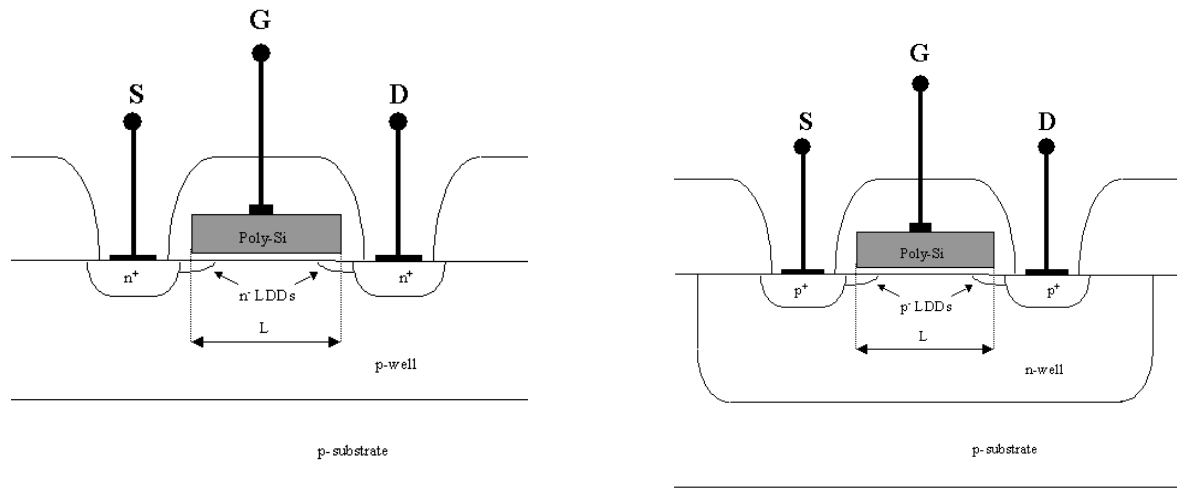


Fig.2.1 Cross-section of the NMOS and PMOS transistors ($n_g=1$).

Example of definition:

$W=90\ \mu\text{m}$, $w_f=5\ \mu\text{m}$, $L=0.35\ \mu\text{m}$, $n_g=18$, $A_d=2.5\ \mu\text{m}^2$, $A_s=2.69\ \mu\text{m}^2$, $P_d=1.0\ \mu\text{m}$, $P_s=1.63\ \mu\text{m}$

W : total gate width, $W=n_g \cdot w_f$.

w_f : width of a single gate finger, $w_f=5$ or $10\ \mu\text{m}$.

L : length of the transistor, $L=0.35\ \mu\text{m}$ (fixed).

n_g : number of gate fingers.

A_d , A_s : drain and source diffusion area.

P_d , P_s : drain and source diffusion perimeter.

2.2 Subcircuit Model

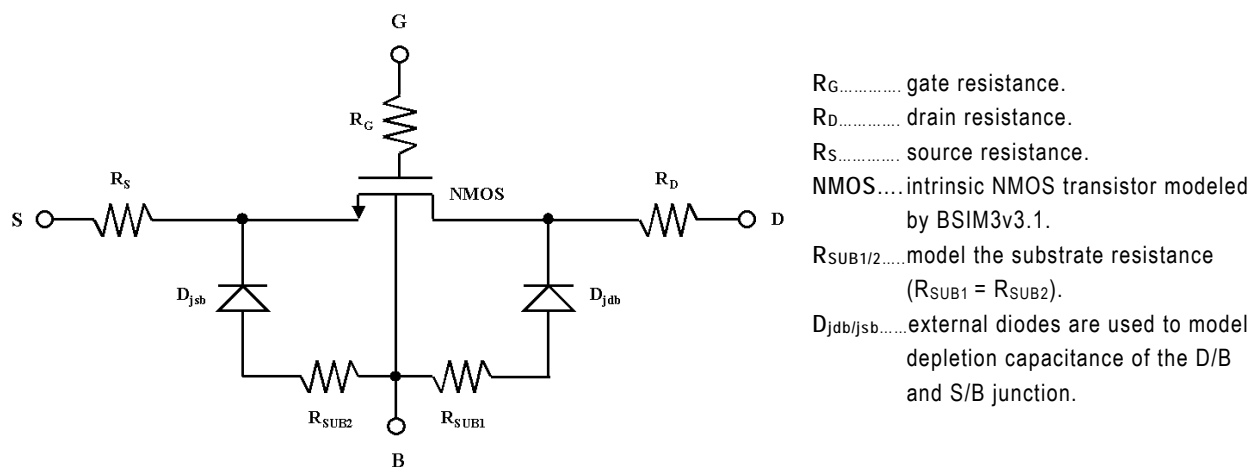


Fig.2.2 RF Subcircuit model of the NMOS transistor. In the case of PMOS the intrinsic transistor is replaced by a PMOS model and the external bulk diodes have opposite direction.

2.3 Main Parameters

wf [μm]	ft [GHz]		fmax [GHz]	
	NMOS	PMOS	NMOS	PMOS
5	28	15	49.9	34.6
10	28	15	36.6	27.9

Table 2.1 ft and fmax of NMOS (at $V_{DS}=3\text{V}$) and PMOS transistors ($V_{DS}=-3\text{V}$).

2.4 Characteristic Curves

2.4.1 Characteristic Curves of NMOS Transistors

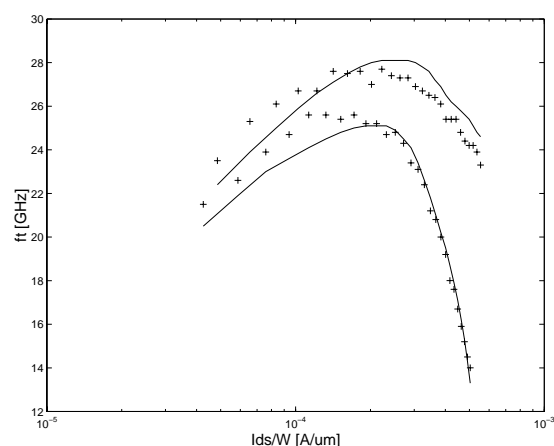


Fig.2.3 Measured and simulated (-) ft versus I_{DS} at $V_{DS}=1.5\text{V}$ (+) and 3V (x) (NMOS ngxwfxL=18x5x0.35).

ENG – 188 Rev. 5.0
0.35 μm CMOS C35 RF SPICE Models

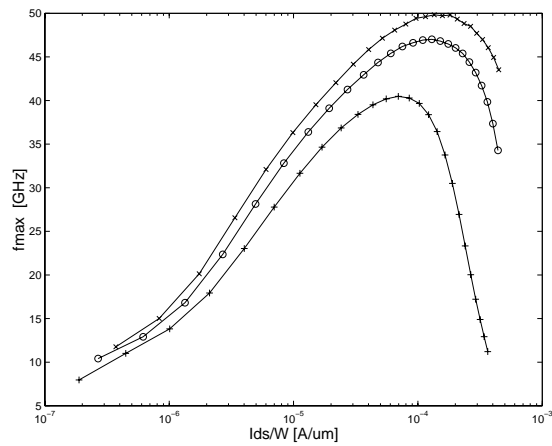


Fig.2.4 Measured and interpolated (-) f_{max} versus I_{ds} at $V_{\text{DS}}=1\text{V}$ (+), 2V (o) and 3V (x) (NMOS $\text{ngxwfxL}=24 \times 5 \times 0.35$).

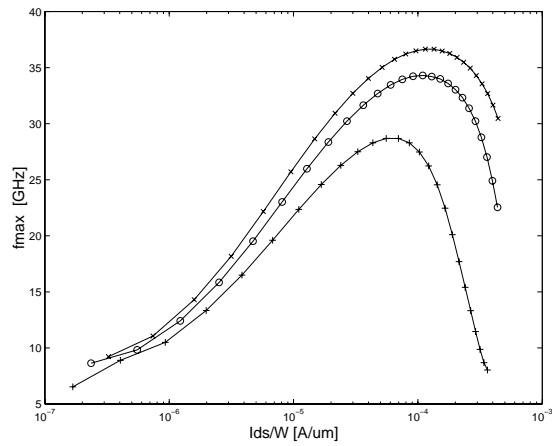


Fig.2.5 Measured and interpolated (-) f_{max} versus I_{ds} at $V_{\text{DS}}=1\text{V}$ (+), 2V (o) and 3V (x) (NMOS $\text{ngxwfxL}=12 \times 10 \times 0.35$).

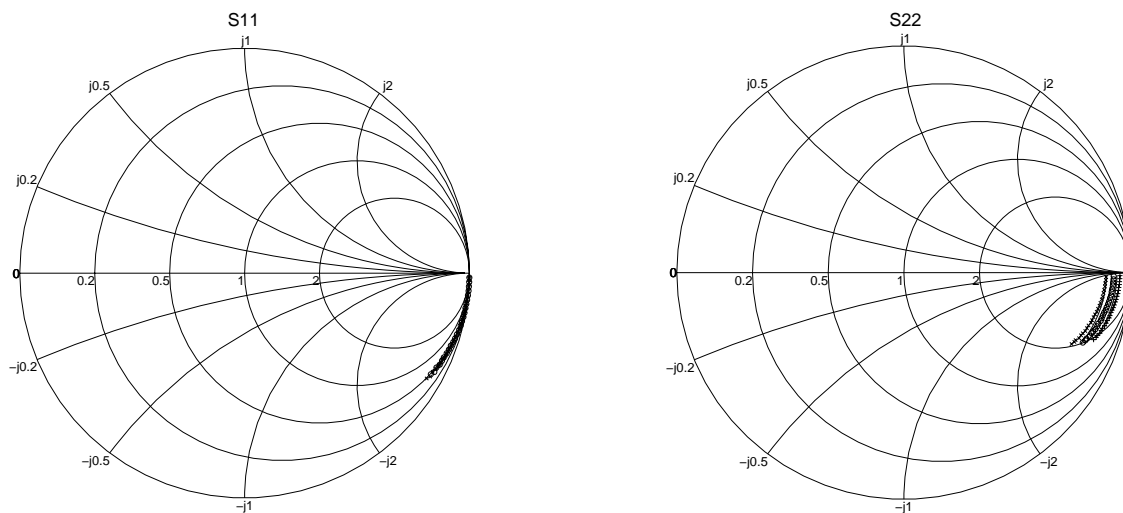


Fig.2.6 Smith chart of measured and simulated (-) S_{11} and S_{22} parameters at $V_{\text{DS}}=3\text{V}$ and $V_{\text{GS}}=1.1\text{V}$ (+), 2.2V (o), 3.3V (x) (NMOS $\text{ngxwfxL}=18 \times 5 \times 0.35$).

ENG – 188 Rev. 5.0
0.35 μm CMOS C35 RF SPICE Models

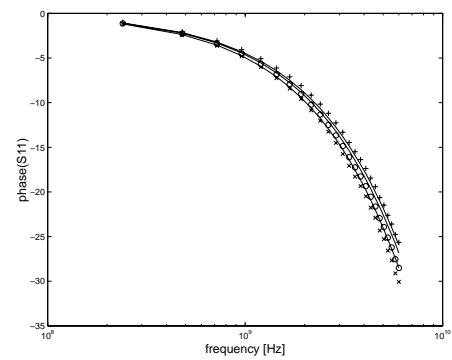
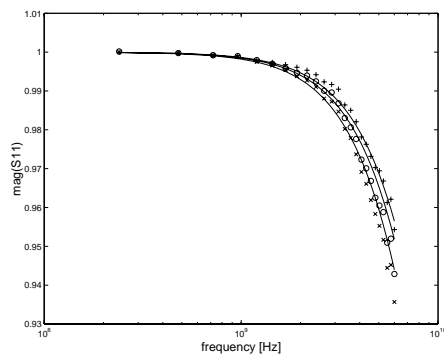


Fig.2.7 Measured and simulated (-) S_{11} (magnitude and phase) at $V_{GS}=1.1\text{V}$ (+), 2.2V (o), 3.3V (x) and $V_{DS}=3\text{V}$ (NMOS ngxwfxL=18x5x0.35).

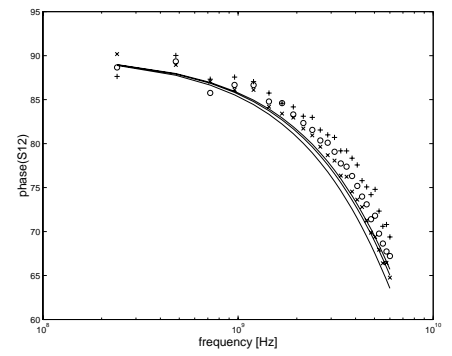
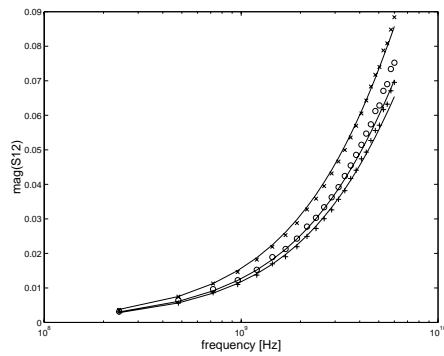


Fig.2.8 Measured and simulated (-) S_{12} (magnitude and phase) at $V_{GS}=1.1\text{V}$ (+), 2.2V (o), 3.3V (x) and $V_{DS}=3\text{V}$ (NMOS ngxwfxL=18x5x0.35).

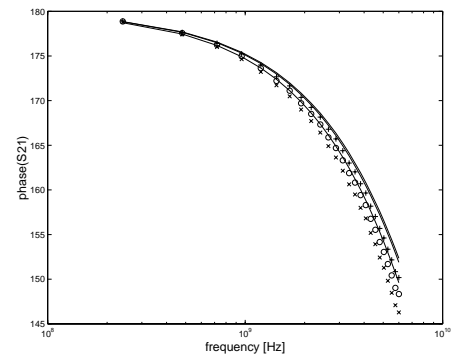
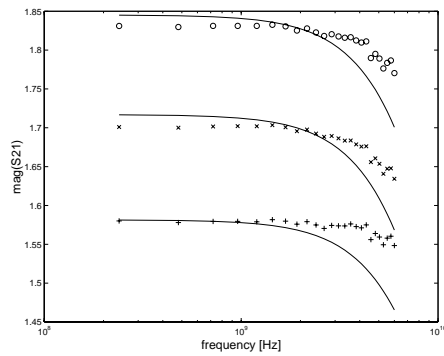


Fig.2.9 Measured and simulated (-) S_{21} (magnitude and phase) at $V_{GS}=1.1\text{V}$ (+), 2.2V (o), 3.3V (x) and $V_{DS}=3\text{V}$ (NMOS ngxwfxL=18x5x0.35).

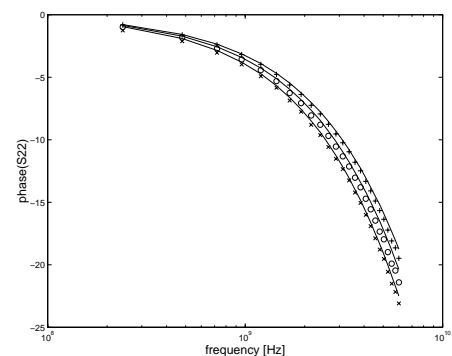
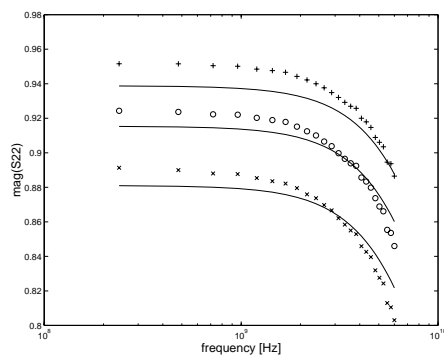


Fig.2.10 Measured and simulated (-) S_{22} (magnitude and phase) at $V_{GS}=1.1\text{V}$ (+), 2.2V (o), 3.3V (x) and $V_{DS}=3\text{V}$ (NMOS ngxwfxL=18x5x0.35).

2.4.2 Characteristic Curves of PMOS Transistors

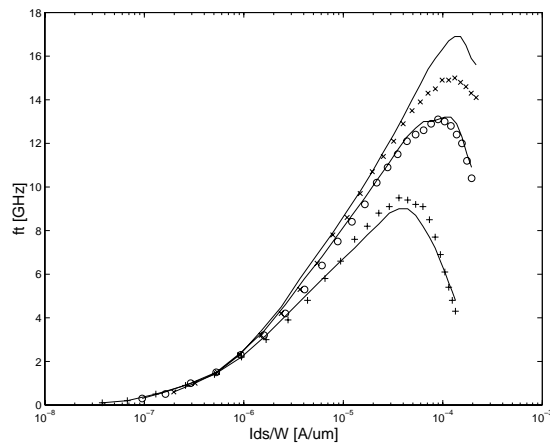


Fig.2.11 Measured and simulated (-) f_t versus I_{ds} at $V_{DS} = -1\text{V}$ (+), -2V (o) and -3V (x) (PMOS ngxwfxL=18x5x0.35).

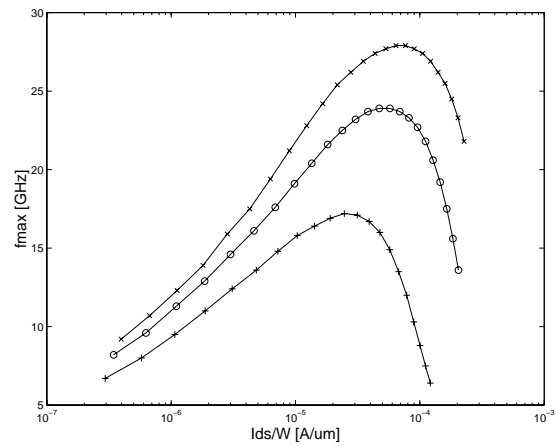
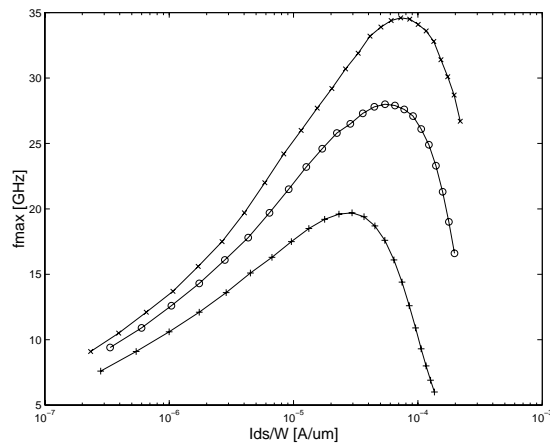


Fig.2.12 Measured and interpolated (-) f_{max} versus I_{ds} at $V_{DS} = -1\text{V}$ (+), -2V (o) and -3V (x) (PMOS ngxwfxL=24x5x0.35 and 12x10x0.35).

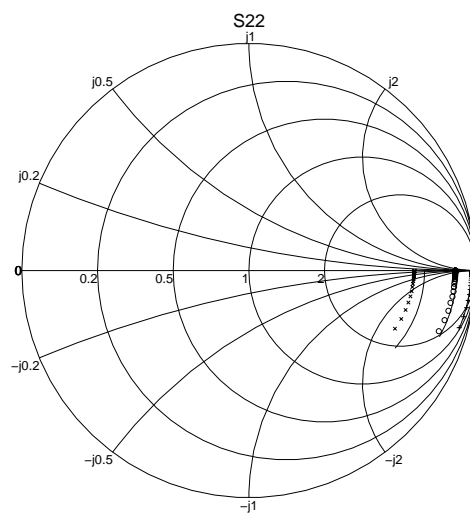
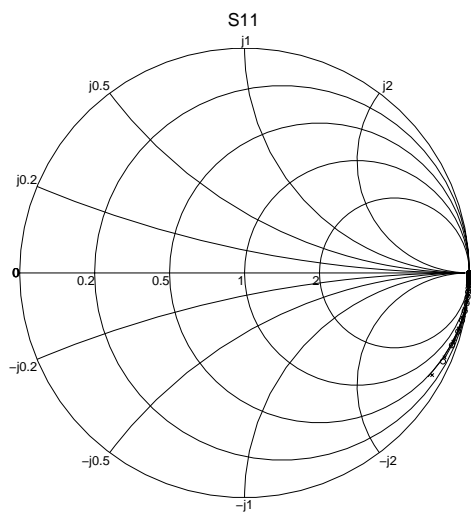


Fig.2.13 Smith chart of measured and simulated (-) S_{11} and S_{22} parameters at $V_{DS} = -2\text{V}$ and $V_{GS} = -1\text{V}$ (+), -2V (o), -3V (x) (PMOS ngxwfxL=18x5x0.35).

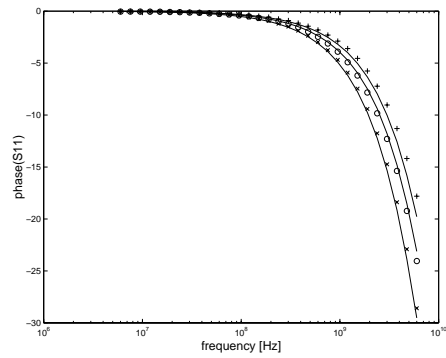
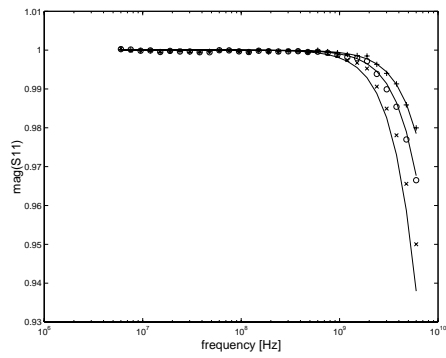


Fig.2.14 Measured and simulated (-) S_{11} (magnitude and phase) at $V_{GS}=-1$ V (+), -2 V (o), -3 V (x) and $V_{DS}=-2$ V (PMOS ngxwfxL=18x5x0.35).

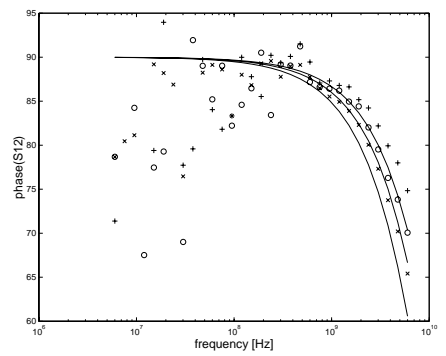
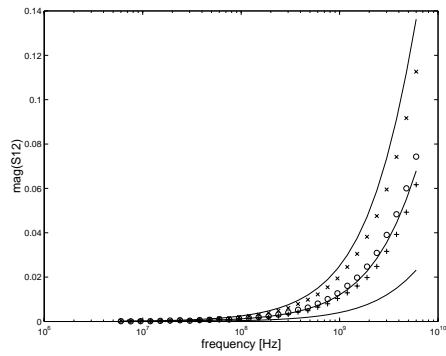


Fig.2.15 Measured and simulated (-) S_{12} (magnitude and phase) at $V_{GS}=-1$ V (+), -2 V (o), -3 V (x) and $V_{DS}=-2$ V (PMOS ngxwfxL=18x5x0.35).

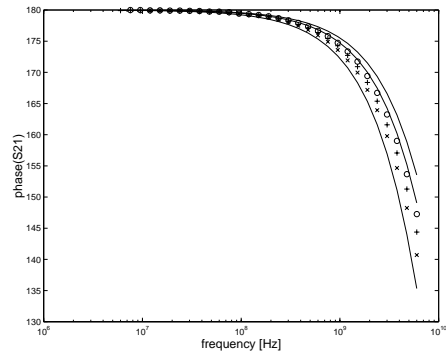
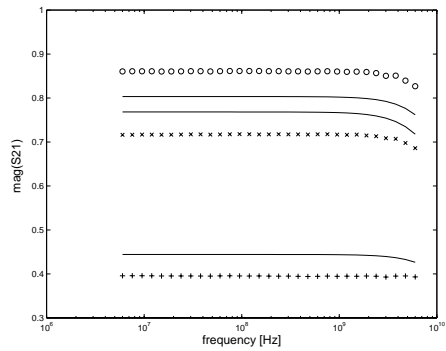


Fig.2.16 Measured and simulated (-) S_{21} (magnitude and phase) at $V_{GS}=-1$ V (+), -2 V (o), -3 V (x) and $V_{DS}=-2$ V (PMOS ngxwfxL=18x5x0.35).

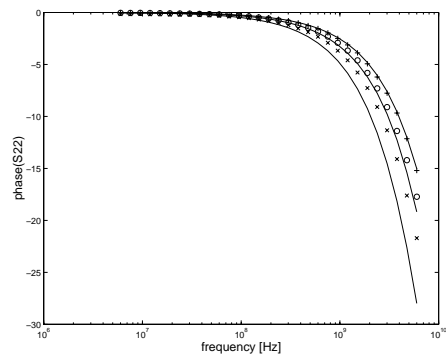
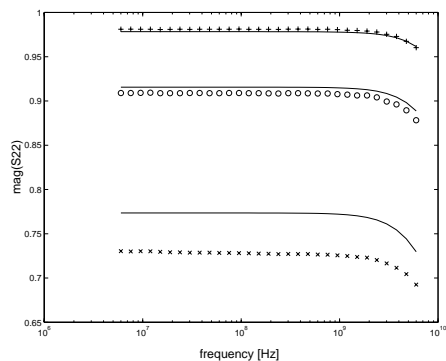


Fig.2.17 Measured and simulated (-) S_{22} (magnitude and phase) at $V_{GS}=-1$ V (+), -2 V (o), -3 V (x) and $V_{DS}=-2$ V (PMOS ngxwfxL=18x5x0.35).

3 MOS Varactor Model (cvar)

An accumulation-mode MOS capacitor implemented as a three-terminal device is available as varactor. The layout of the device is composed of parallel connected small capacitors. The capacitance-voltage characteristics is modeled by the gate-bulk capacitance of a PMOS transistor using the BSIM3v3.2 model. In addition the subcircuit model of the varactor contains parasitic resistors and diodes used for n-well/p-substrate junction capacitance modeling [1]. The model scales with the total width of the device.

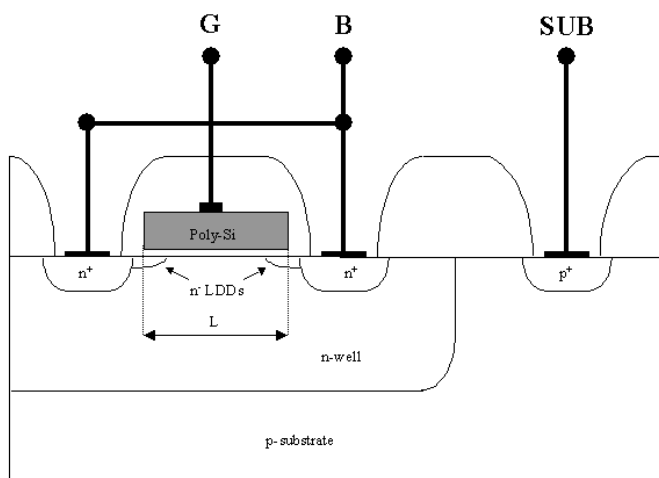
The model is valid in the following range:

frequency range: few kHz – 6 GHz

Total width: 100 - 1000 μm

Layout: Array of row*col unit capacitors (see Fig. 3.2), preferred col/row ratio is 1 – 5.

3.1 Cross-Section, Layout and Device Definition



Terminals:

G : gate

B : bulk (n-well)

SUB : p-substrate (grounded)

MOS capacitor electrodes: G and B

Well diode electrodes: SUB (anode) and B (cathode)

Fig.3.1 Cross-section of the accumulation-mode MOS varactor.

Example of definition:

W=950.4 μm , wseg=6.6 μm , L=0.65 μm , row=9, col=16, AW=2016 μm^2 , PW=201 μm , M =1

W: total width of the varactor, $W = \text{row} * \text{col} * \text{wseg}$.

The layout of the MOS varactor consists of small parallel connected MOS capacitors in order to increase the quality (Q).

The capacitance can be adjusted by setting W. This can be done by setting row and col.

wseg: width of a segment, wseg=6.6 μm (fixed).

L: length of the varactor (spacing of the n-well contacts), L=0.65 μm (fixed).

row: number of rows in vertical direction.

col: number of columns in horizontal direction.

AW: area of the n-well. AW and PW strongly depend on the pre-defined layout (Cadence pcell) of the varactor consisting of an array of rows and columns and can be calculated as follows:

$$AW = (0.8 * \text{row} + 6.6 * \text{row} + 0.8 * (\text{row} - 1) - 0.1 * 2) * (0.3 * 2 + 0.85 * 2 + 0.65 * \text{col} + 1.0 * (\text{col} - 1)) * 1e-12 \text{ m}^2$$

PW: perimeter of the n-well. PW can be calculated as follows:

$$PW = 2 * (0.8 * \text{row} + 6.6 * \text{row} + 0.8 * (\text{row} - 1) - 0.1 * 2 + 0.3 * 2 + 0.85 * 2 + 0.65 * \text{col} + 1.0 * (\text{col} - 1)) * 1e-6 \text{ m}$$

M: number of devices in parallel, M = 1 (fixed)

In aid of layout design the layout structure and geometrical data of the test-structures are shown in Fig. 3.2 and in Table 3.1.

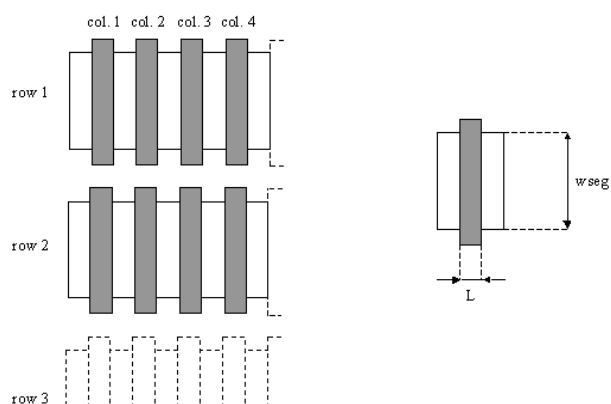


Fig.3.2 Layout structure of the MOS varactor.

W [μm]	Row	Col	L [μm]	Cmin [pF]	Cmax [pF]
950.4	9	16	0.65	0.81	2.97
633.6	6	16	0.65	0.54	1.98
316.8	3	16	0.65	0.27	0.99
158.4	3	8	0.65	0.14	0.49

Table 3.1 Geometric dimensions and measured C_{min} and C_{max} values of the test-structures.

3.2 Subcircuit Model

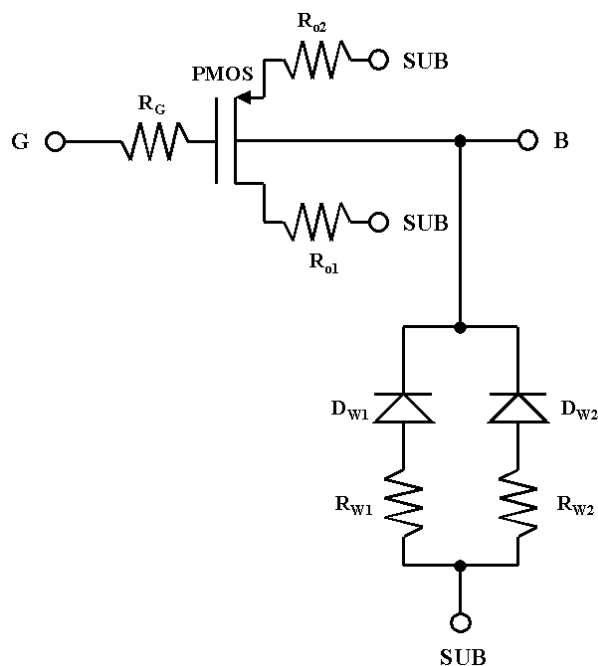


Fig.3.3 Subcircuit model of the accumulation-mode MOS varactor.

- R_G series resistance of the MOS capacitor
- PMOS.... the gate-bulk capacitance of a PMOS transistor is used to model (BSIM3v3.2) the MOS capacitance between G and B
- $R_{o1/2}$ prevent the gate-bulk capacitance from rising to C_{max} in inversion (MOS capacitor vs. MOS transistor)
- $R_{W1/2}$ model the series resistance of the well
- $D_{W1/2}$ diodes are used to model the depletion capacitance of the well

3.3 Main Parameters

Important electrical parameters are calculated using the impedance between gate and bulk ($Z=1/y_{11}$).

MOS Capacitance:
$$C = \frac{1}{-\omega \text{Im}(Z)}$$

Series Resistance:
$$R = \text{Re}(Z) = R_g$$

Capacitance Tuning Range:
$$\gamma = \pm \frac{C_{\max} - C_{\min}}{C_{\max} + C_{\min}}$$

Quality Factor:
$$Q = \frac{|\text{Im}(Z)|}{|\text{Re}(Z)|} = \left| -\frac{1}{\omega RC} \right|$$

where $\omega=2\pi f$ (f: frequency), $\text{Re}(Z)$ and $\text{Im}(Z)$ are the real and imaginary part of the impedance.

Notice: The C and R characteristics are independent of frequency. Q depends on frequency. The strong deviation in the Q-V characteristics is due to the approximation of the nonlinear series resistance with a constant resistance.

W [μm]	C_{\max}/C_{\min}	γ [%]	Q_{\min} (at 2.4 GHz)
950.4	3.65	57.0	79.7
633.6	3.66	57.1	58.0
316.8	3.68	57.3	42.6
158.4	3.65	57.0	41.4

Table 3.2 Measured C_{\max}/C_{\min} ratio, capacitance tuning range and minimum quality factor.

3.4 Characteristic Curves

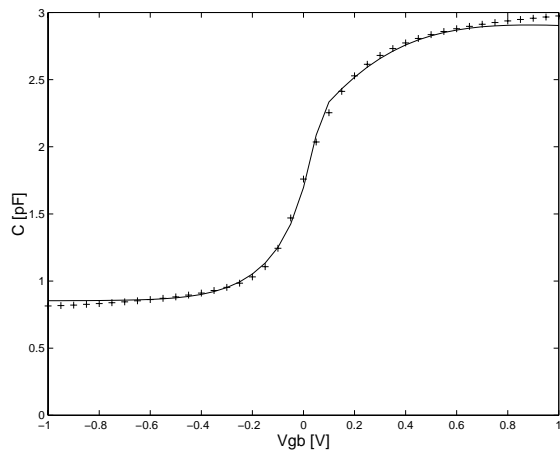


Fig.3.4 Measured (+) and simulated (-) C-V characteristics ($W=950 \mu\text{m}$).

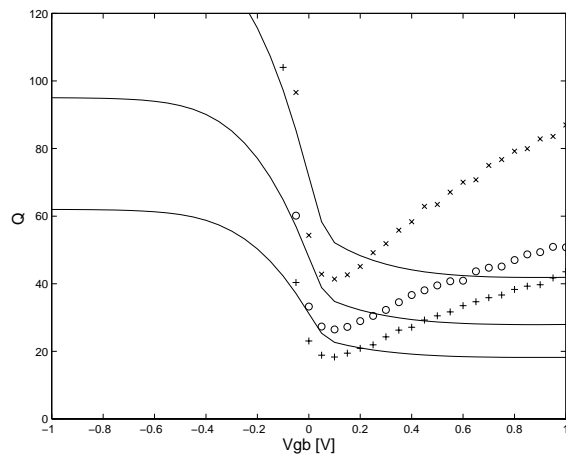


Fig.3.5 Measured and simulated (-) Q of the $W=158 \mu\text{m}$ varactor as a function of V_{GB} at 2.4 GHz (x), at 3.6 GHz (o) and at 5.5 GHz (+).

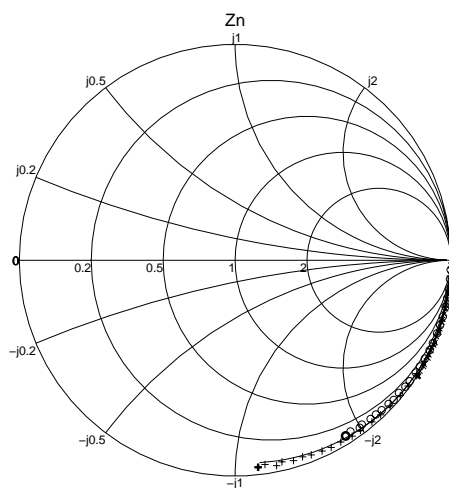


Fig.3.6 Measured and simulated (-) normalized gate to bulk impedance $Z_n = (Z - 50) / (Z + 50)$ at $V_G = -0.5$ V (x), 0 V (o), 0.5 V (+) and $V_B = 0$ V ($W=158 \mu\text{m}$).

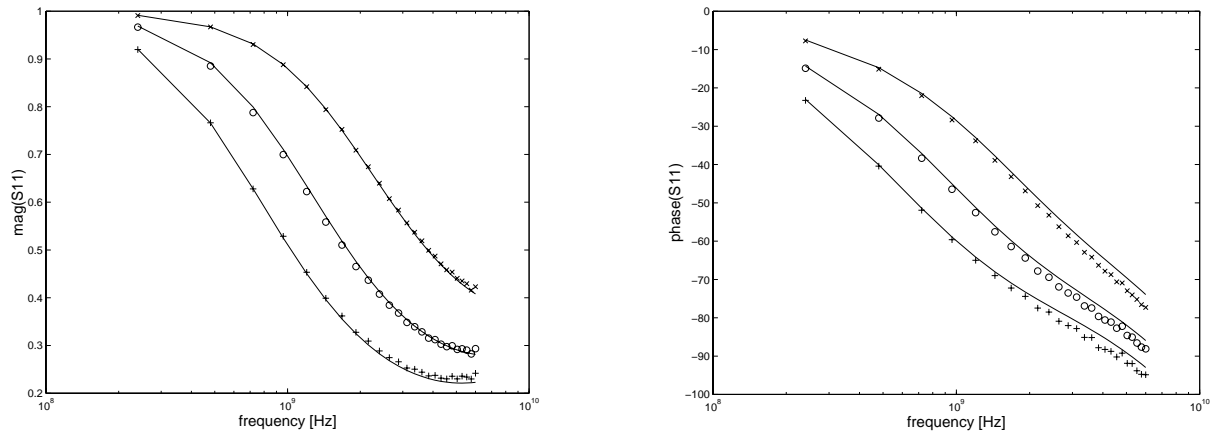


Fig.3.7 Measured and simulated (-) S_{11} (magnitude and phase) at $V_G = -0.5\text{V}$ (x), 0V (o), 0.5V (+) and $V_B = 0\text{V}$ ($W = 950\text{ }\mu\text{m}$).

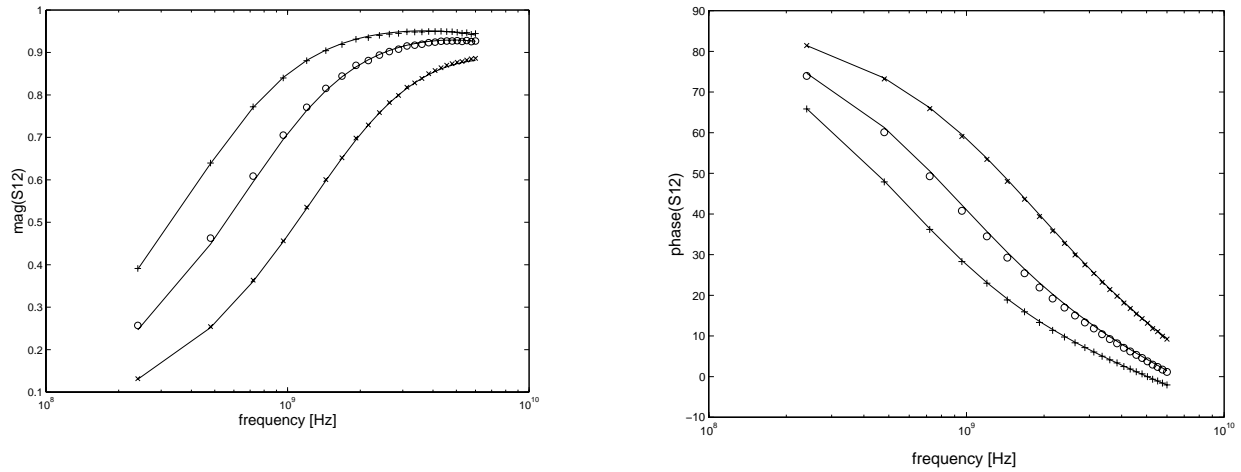


Fig.3.8 Measured and simulated (-) S_{12} (magnitude and phase) at $V_G = -0.5\text{V}$ (x), 0V (o), 0.5V (+) and $V_B = 0\text{V}$ ($W = 950\text{ }\mu\text{m}$).

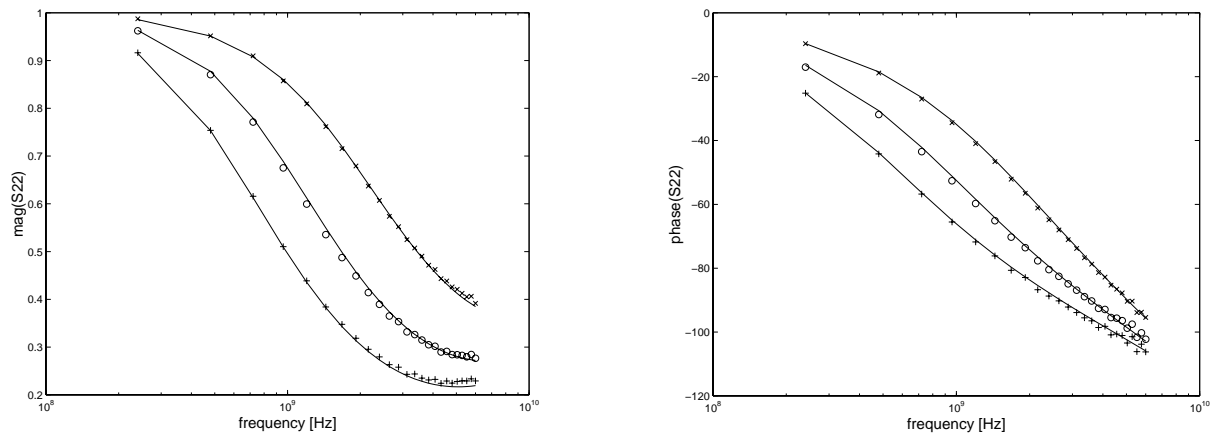


Fig.3.9 Measured and simulated (-) S_{22} (magnitude and phase) at $V_G = -0.5\text{V}$ (x), 0V (o), 0.5V (+) and $V_B = 0\text{V}$ ($W = 950\text{ }\mu\text{m}$).

[1] K. Molnar, G. Rappitsch, Z. Huszka, and E. Seebacher, "MOS varactor modeling with a subcircuit utilizing the BSIM3v3 model," IEEE Transactions on Electron Devices, vol.49, pp. 1206-1211, July 2002.

4 Inductor Models (STxxxAyyyB)

austriamicrosystems provides three inductor libraries (please refer to 1.2 Process Family):

- 1.) 3 metal (valid for the 3 metal processes)
- 2.) 4 metal (valid for 4 metal module)
- 3.) thick metal (valid for thick metal module).

The 3 metal library consists of 23 square inductors with values ranging from 1.3 nH up to 20 nH and 6 square symmetric inductors with values ranging from 1.4 nH to 2.8 nH. The 4 metal library contains 7 square inductors with values ranging from 1.4 nH to 9.1 nH. The thick metal library is composed of 14 square inductors covering the range from 1.1 nH to 13.3 nH. The layout of the inductors is fixed. All inductors are modeled with a lumped RLC equivalent circuit.

Nomenclature of inductors:

STxxxAyyyB:

- T..... inductor type (P: square, Y: square symmetric)
- xxx..... nominal port 1 drive inductance multiplied by 10 in nH
- A..... inductor layout (S: single structure, C: multilayer structure)
- yyy..... outer dimension of inductor in μm
- B..... process (C: 3 metal process, D: 4 metal module, T: thick metal module)

e.g. SP025C200C: inductance~2.5 nH, multilayer structure, inductor area=200x200 μm^2 , 3 metal process
SY014C165C: inductance~1.4 nH, multilayer structure, inductor area=165x165 μm^2 , 3 metal process

4.1 Subcircuit Model

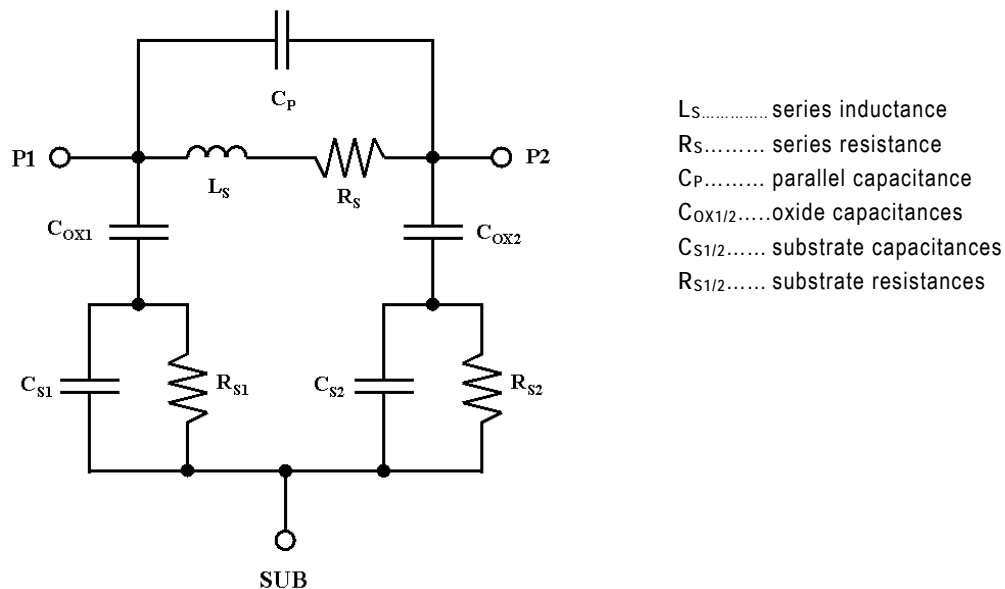


Fig.4.1 The inductor subcircuit model.

Note:

The models are optimized for single ended operation. P1 always denotes the terminal with the higher quality factor.

4.2 Main Parameters

Important electrical parameters are summarized for P1 drive operation calculated from the impedance $Z=1/y_{11}$.

Effective Series Inductance: $L = \frac{\text{Im}(Z)}{\omega}$

Effective Series Resistance: $R = \text{Re}(Z)$

Quality Factor: $Q = \frac{|\text{Im}(Z)|}{|\text{Re}(Z)|}$

where $\omega=2\pi f$ (f: frequency), $\text{Re}(Z)$ and $\text{Im}(Z)$ are the real and imaginary part of the impedance.

4.2.1 Main Parameters of 3 Metal Inductors

Inductor	Inductance [nH]			Qmax	Q		f _{RES} [GHz]
	L _s	@1GHz	@2GHz		@1GHz	@2GHz	
SP014S300C	1.32	1.32	1.32	6.4@2.5GHz	4.2	6.0	>10
SP018S300C	1.86	1.87	1.90	6.0@2.2GHz	4.2	5.9	>10
SP020S180C	1.99	1.98	1.97	5.3@3.5GHz	2.8	4.7	>10GHz
SP023S200C	2.13	2.14	2.15	4.8@2.3GHz	3.5	4.7	>10
SP025C200C	2.33	2.35	2.46	6.1@3.0GHz	3.6	5.4	6.7
SP026S200C	2.59	2.60	2.64	5.2@3.0GHz	3.1	4.7	>10GHz
SP028S300C	2.61	2.62	2.64	5.6@1.4GHz	5.2	5.1	9.2
SP028C200C	2.82	2.86	2.93	4.3@3.0GHz	2.4	3.8	8.6
SP030C200C	3.00	3.02	3.09	4.0@3.6GHz	1.9	3.2	>10GHz
SP037S180C	3.73	3.76	3.83	5.0@3.3GHz	2.4	4.0	>10GHz
SP038S300C	3.82	3.85	3.99	4.1@1.2GHz	3.9	3.5	7.3
SP040C200C	3.91	4.00	4.25	3.9@2.1GHz	2.8	3.8	>10GHz
SP040C300C	3.85	4.18	5.10	5.4@1.9GHz	4.5	5.3	3.7
SP045C200C	4.52	4.70	5.50	4.0@1.7GHz	3.5	3.7	3.9
SP047S180C	4.71	4.79	4.96	4.6@2.7GHz	2.5	4.2	>10GHz
SP050S155C	5.30	5.38	5.57	4.2@3.0GHz	2.1	3.6	>10GHz
SP051C300C	5.11	5.7	8.8	3.8@1.1GHz	3.7	2.4	2.8
SP068C300C	6.73	8.0	16.0	3.6@0.9GHz	3.5	0.5	2.1
SP090S155C	9.05	9.29	9.83	3.2@2.6GHz	3.0	2.9	8.0GHz
SP090C200C	8.83	10.3	18.2	3.4@1.2GHz	3.3	2.1	2.6
SP112C300C	11.3	17.1	-	3.2@0.8GHz	2.9	-	1.6
SP140C200C	14.2	18.3	-	2.9@1.0GHz	2.9	-	2.0
SP200C200C	19.9	29.9	-	2.5@0.9GHz	2.3	-	1.6
SY014C165C	1.43	1.43	1.42	6.2@3.5GHz	3.3	5.1	>10GHz
SY015C200C	1.48	1.47	1.46	5.4@3.1GHz	3.2	4.7	>10GHz
SY016C180C	1.57	1.57	1.57	6.5@3.4GHz	3.5	5.4	>10GHz
SY017C165C	1.70	1.70	1.70	5.3@3.1GHz	3.2	4.7	>10GHz
SY019C180C	1.92	1.92	1.91	5.3@2.9GHz	3.4	4.9	>10GHz
SY028C160C	2.81	2.82	2.89	5.5@3.2GHz	2.8	4.7	>10GHz

Table 4.1 Extracted L, maximum Q (Qmax) and resonance frequencies (f_{RES}) of 3 metal inductors.

Note: Results are valid for 3 metal processes according to 1.2 (Process Family)

4.2.2 Main Parameters of 4 Metal Inductors

Inductor	Inductance [nH]			Qmax	Q		f _{RES} [GHz]
	L _s	@2.4GHz	@5.0GHz		@2.4GHz	@5.0GHz	
SP014S300D	1.37	1.34	1.38	6.8@3.8GHz	6.1	6.2	>6
SP020S180D	2.01	1.99	2.04	5.8@5.0GHz	4.5	5.7	>6
SP026S200D	2.60	2.64	2.83	5.7@3.8GHz	4.7	5.3	>6
SP037S180D	3.77	3.87	4.30	5.1@4.3GHz	3.9	4.9	>6
SP047S180D	4.78	5.01	5.81	4.8@3.8GHz	4.1	4.1	>6
SP050S155D	5.52	5.62	6.47	4.4@3.8GHz	3.4	4.1	>6
SP090S155D	9.15	9.98	12.7	3.5@3.3GHz	3.3	2.5	>6

Table 4.2 Extracted L, Qmax and resonance frequencies of 4 metal inductors.

Note: Results are valid for metal 4 module according to 1.2 (Process Family)

4.2.3 Main Parameters of Thick Metal Inductors

Inductor	Inductance [nH]			Qmax	Q		f _{RES} [GHz]
	L _s	@2.4GHz	@5.0GHz		@2.4GHz	@5.0GHz	
SP011S200T	1.07	1.04	1.05	11.9@4.4GHz	8.7	11.8	>6
SP015S250T	1.52	1.49	1.58	11.7@3.9GHz	9.6	10.2	>6
SP020S250T	2.02	2.04	2.17	10.4@3.9GHz	7.9	9.8	>6
SP021S200T	2.10	2.10	2.20	9.9@3.9GHz	7.8	9.3	>6
SP024S250T	2.42	2.42	2.75	9.6@2.70GHz	9.3	6.5	>6
SP031S250T	3.07	3.17	3.63	8.9@3.0GHz	8.4	6.6	>6
SP033S150T	3.25	3.32	3.52	9.4@4.33GHz	6.9	9.0	>6
SP037S250T	3.67	3.82	4.58	9.4@2.70GHz	9.0	6.2	>6
SP047S250T	4.66	4.90	5.98	8.3@3.7GHz	7.2	6.4	>6
SP049S300T	4.85	5.30	8.13	8.8@2.46GHz	8.6	3.7	>6
SP060S300T	6.00	6.59	10.09	7.2@3.0GHz	6.8	4.3	>6
SP073S250T	7.25	8.11	12.20	7.7@2.5GHz	7.5	3.2	>6
SP100S250T	10.02	12.08	19.23	7.2@2.0GHz	6.8	1.1	6
SP133S300T	13.30	19.06	-	6.7@1.7GHz	5.5	-	4.3

Table 4.3 Extracted L, Qmax and resonance frequencies of thick metal inductors.

Note: Results are valid for thick metal module according to 1.2 (Process Family)

4.3 Characteristic Curves

4.3.1 Characteristic Curves of 3 Metal Inductors

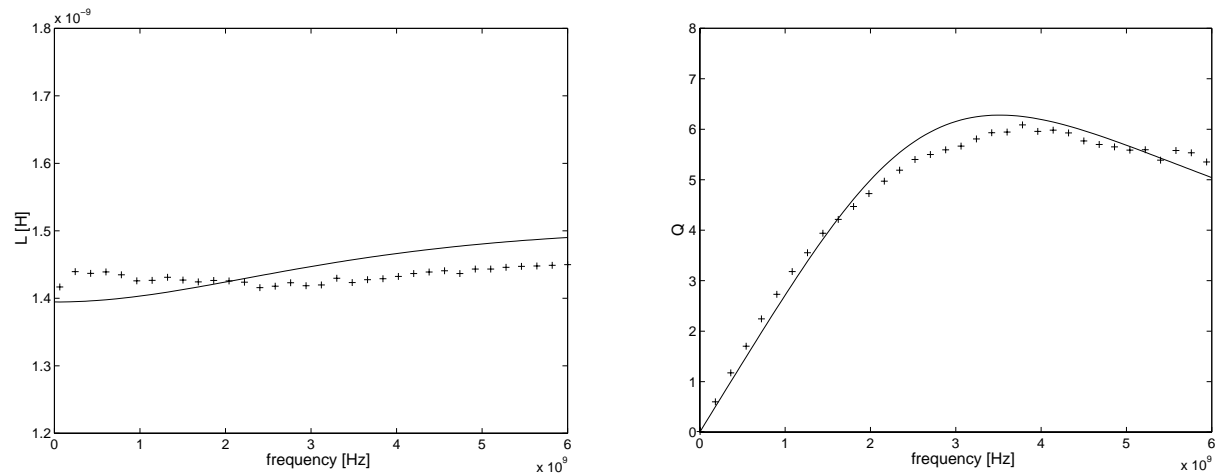


Fig. 4.2 Measured (x) and simulated (-) effective series inductance and quality factor of spiral SY014C165C as a function of frequency.

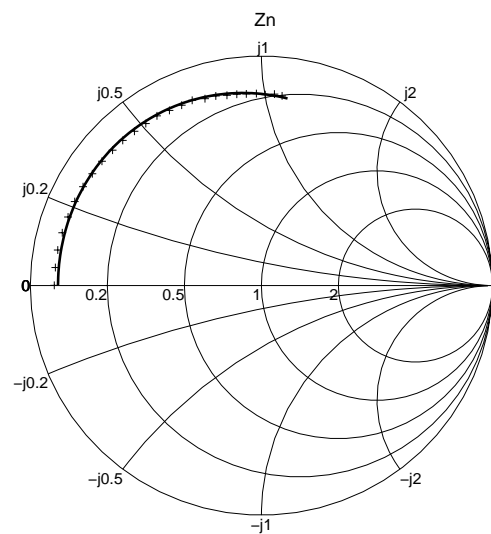


Fig.4.3 Measured (x) and simulated (-) normalized impedance $Z_n=(Z-50)/(Z+50)$ of spiral SY014C165C.

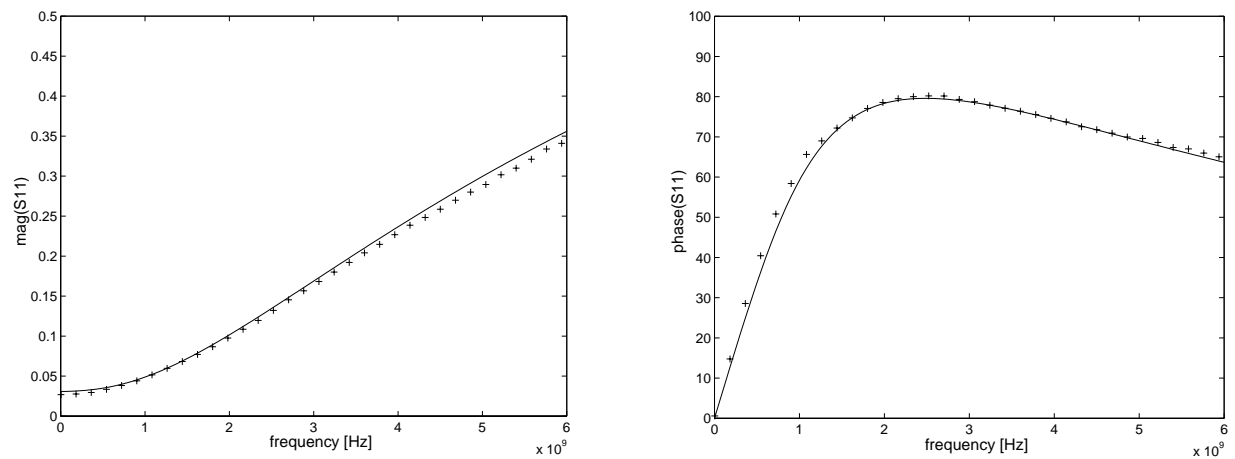


Fig.4.4 Measured (x) and simulated (-) S_{11} (magnitude and phase) of spiral SY014C165C.

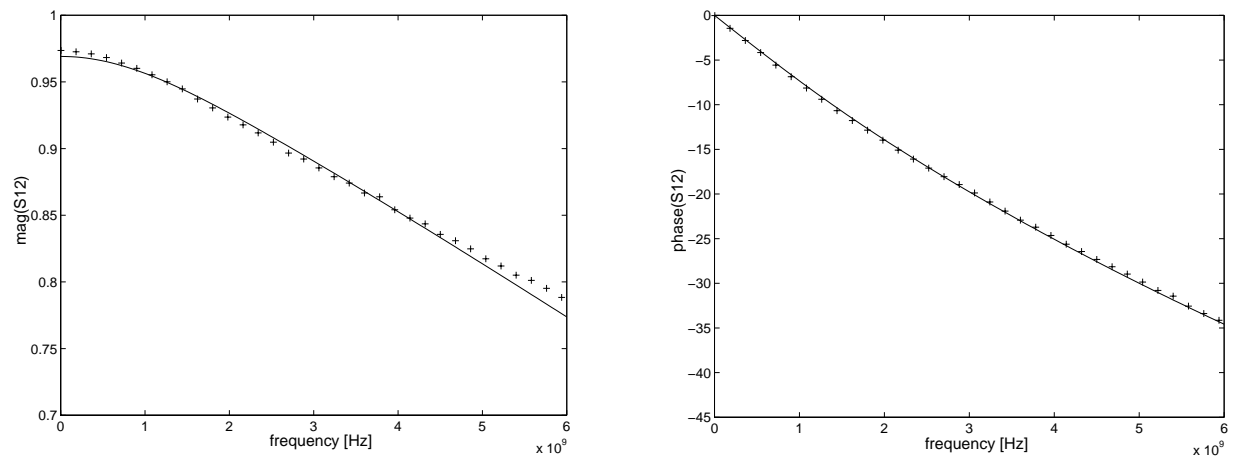


Fig.4.5 Measured (x) and simulated (-) S_{12} (magnitude and phase) of spiral SY014C165C.

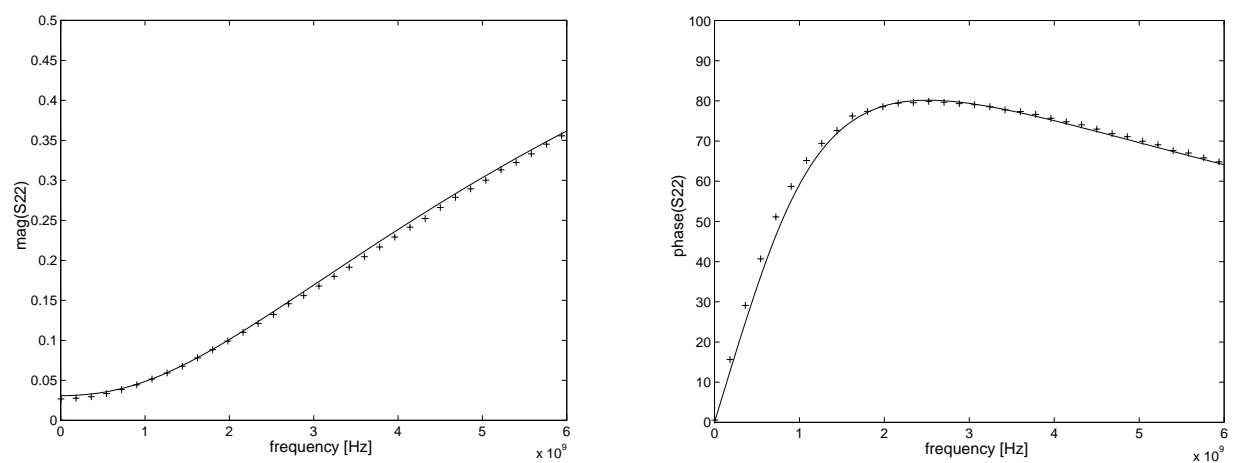


Fig.4.6 Measured (x) and simulated (-) S_{22} (magnitude and phase) of spiral SY014C165C.

4.3.2 Characteristic Curves of 4 Metal Inductors

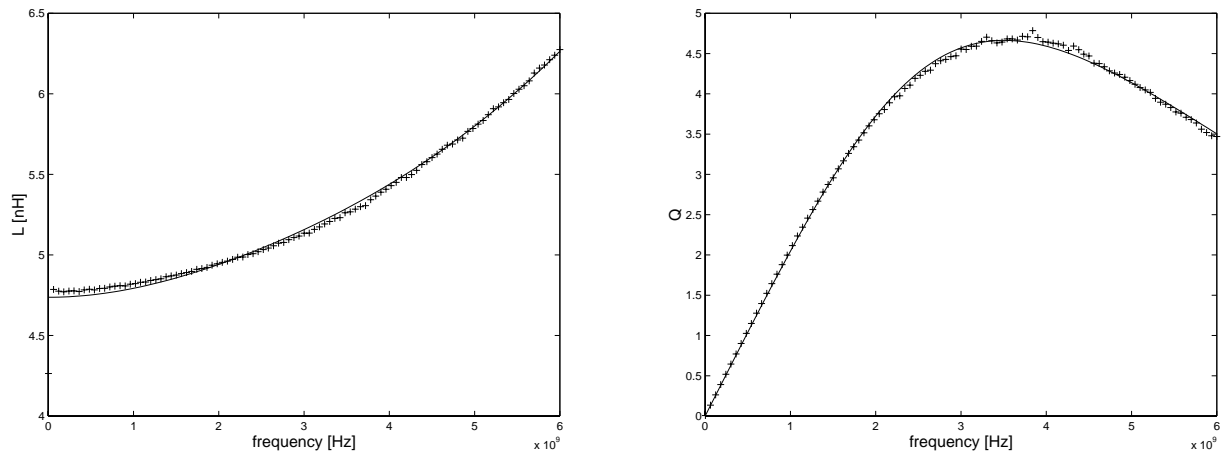


Fig. 4.7 Measured (x) and simulated (-) effective series inductance and quality factor of spiral SP047S180D as a function of frequency.

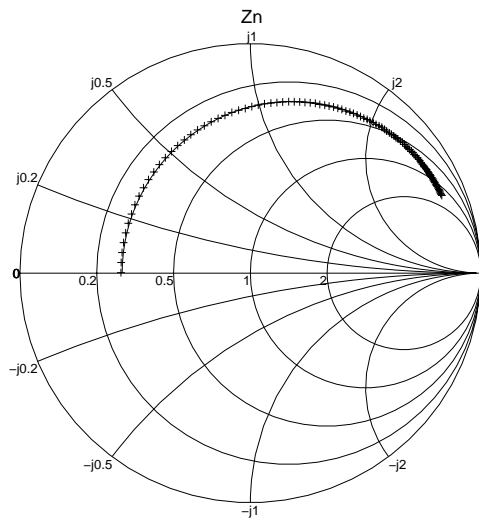


Fig.4.8 Measured (x) and simulated (-) normalized impedance $Z_n=(Z-50)/(Z+50)$ of spiral SP047S180D.

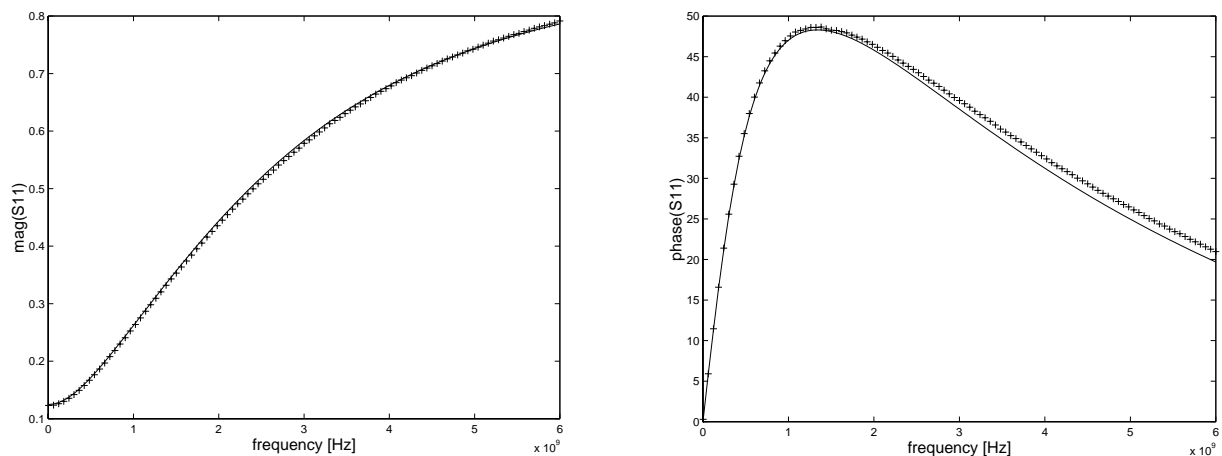


Fig.4.9 Measured (x) and simulated (-) S_{11} (magnitude and phase) of spiral SP047S180D.

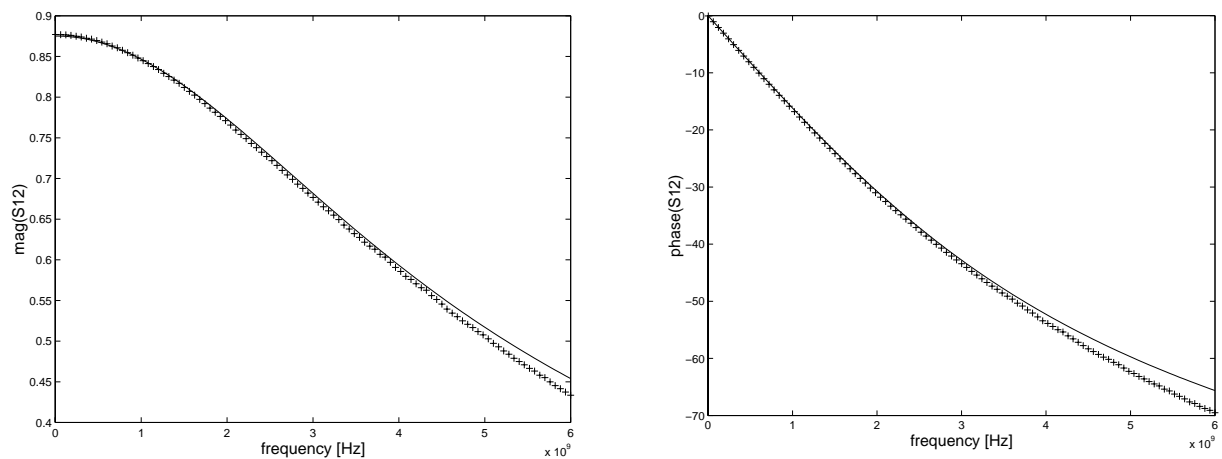


Fig.4.10 Measured (x) and simulated (-) S_{12} (magnitude and phase) of spiral SP047S180D.

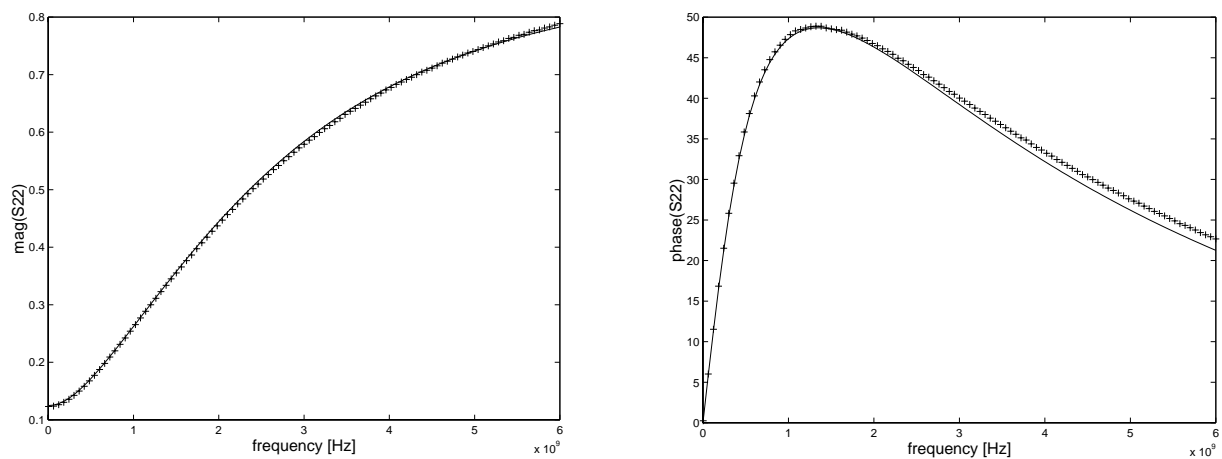


Fig.4.11 Measured (x) and simulated (-) S_{22} (magnitude and phase) of spiral SP047S180D.

4.3.3 Characteristic Curves of Thick Metal Inductors

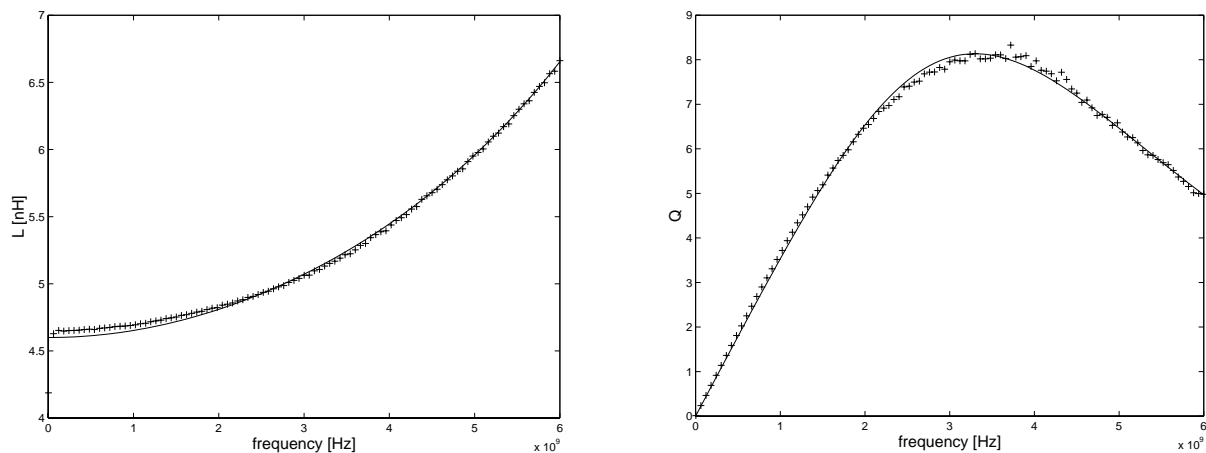


Fig. 4.12 Measured (x) and simulated (-) effective series inductance and quality factor of spiral SP047S250T as a function of frequency.

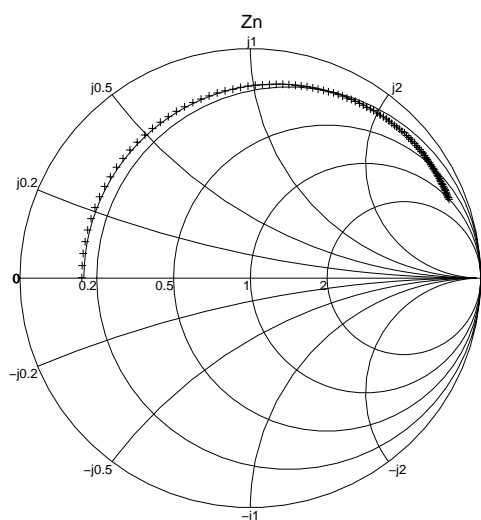


Fig.4.13 Measured (x) and simulated (-) normalized impedance $Z_n=(Z-50)/(Z+50)$ of spiral SP047S250T.

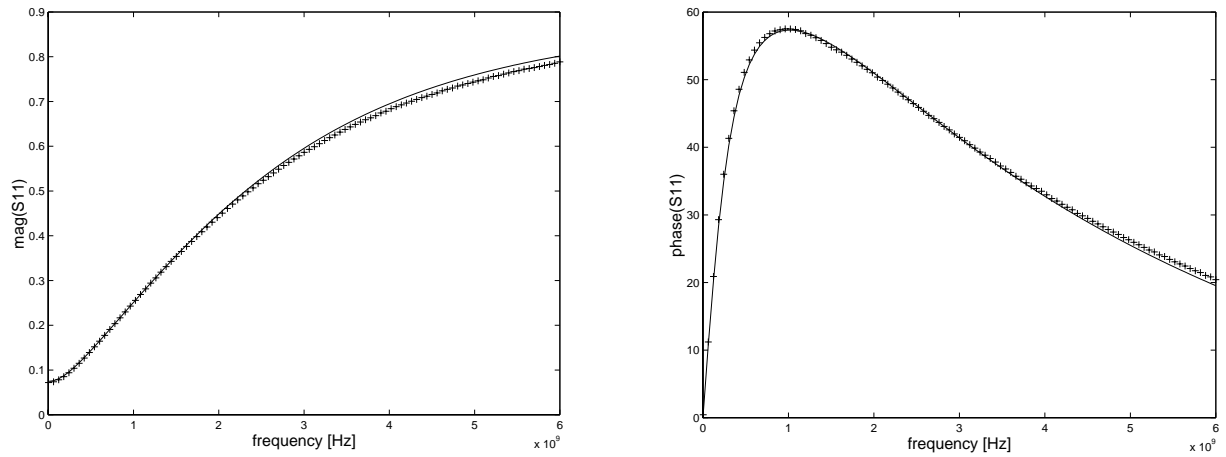


Fig.4.14 Measured (x) and simulated (-) S_{11} (magnitude and phase) of spiral SP047S250T.

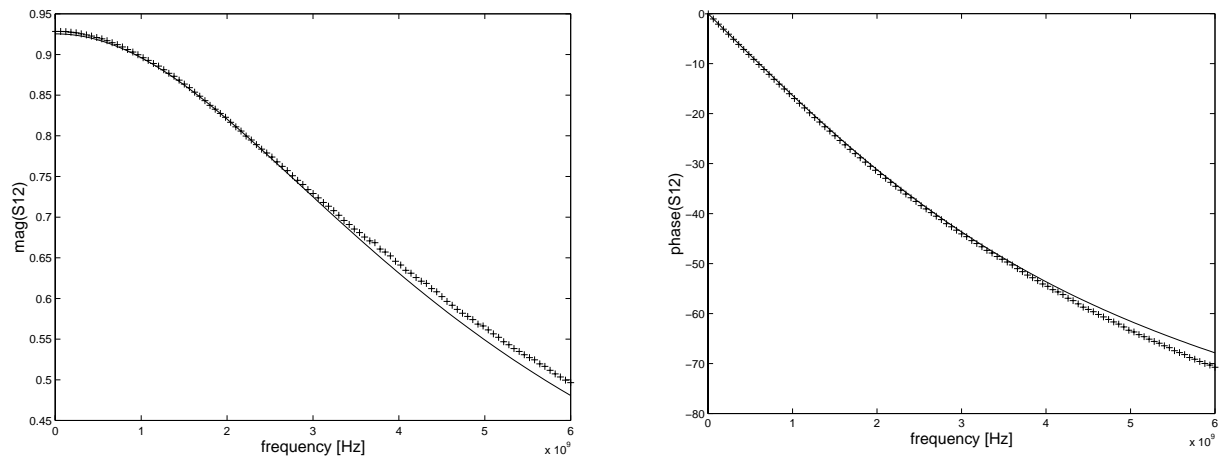


Fig.4.15 Measured (x) and simulated (-) S_{12} (magnitude and phase) of spiral SP047S250T.

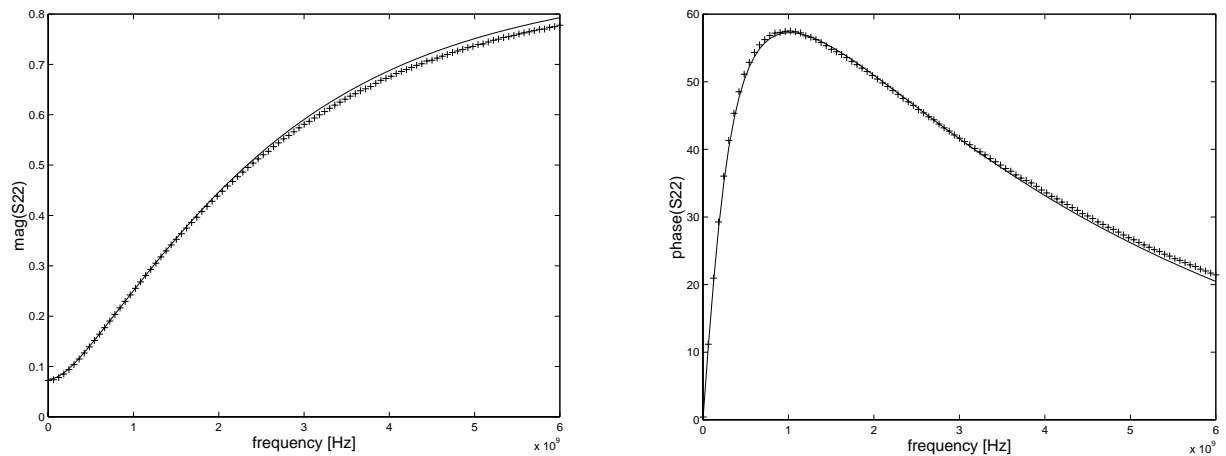


Fig.4.16 Measured (x) and simulated (-) S_{22} (magnitude and phase) of spiral SP047S250T.

5 Differential Inductor Models (DlxxPT)

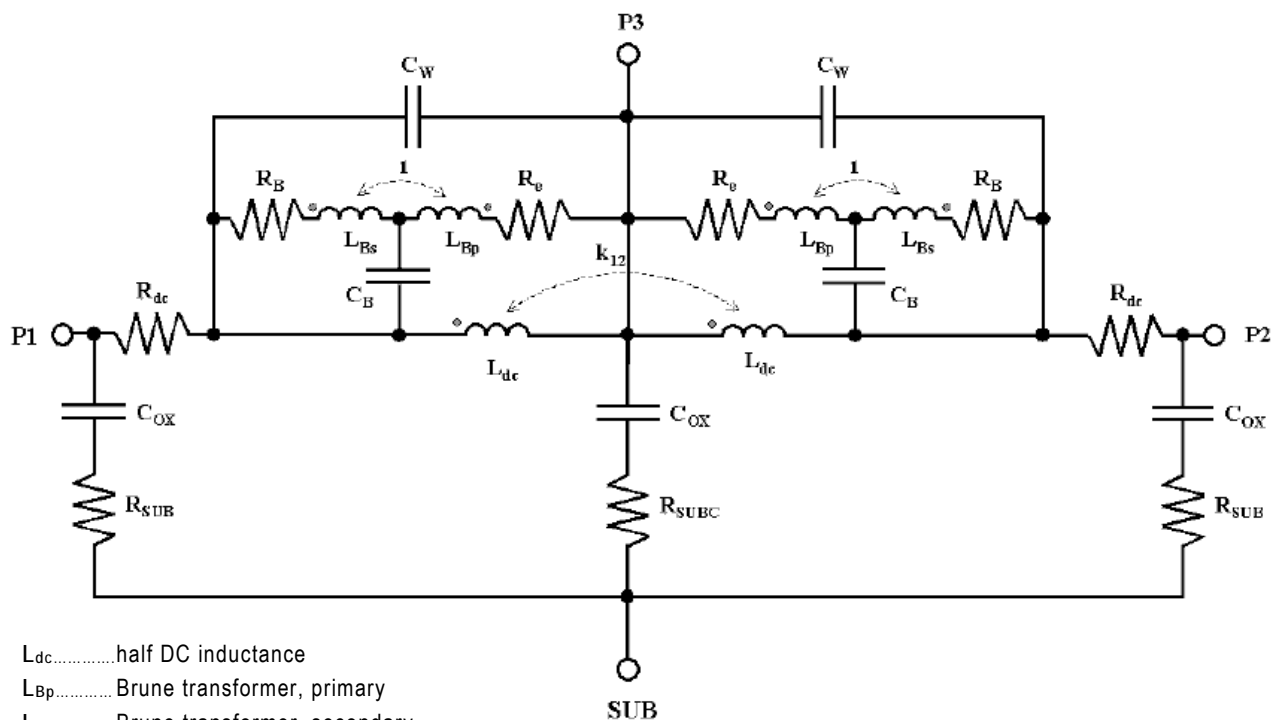
austriamicrosystems provides a differential inductor library available for the thick metal module (please refer to 1.2 Process Family). The library consists of 10 octagonal inductors with values ranging from 1.5 nH up to 6 nH. The layout of the inductors is fixed. All inductors are modeled with a lumped RLC equivalent circuit [2].

Nomenclature of differential inductors:

DlxxPT:

- xx..... nominal differential inductance multiplied by 10 in nH
- P..... poly shield
- T..... process (T: thick metal module)

5.1 Subcircuit Model



- L_{dc} half DC inductance
- L_{Bp} Brune transformer, primary
- L_{Bs} Brune transformer, secondary
- k_{12} coupling coefficient of half inductors
- R_{dc} half DC resistance
- R_B Brune resistance
- R_e Brune entry resistor
- C_W half winding capacitance
- C_B Brune capacitance
- $C_{OX/C}$ outer and center oxide capacitances
- $R_{SUB/C}$ outer and center substrate resistances

Fig.5.1 The differential inductor subcircuit model.

5.2 Main Parameters

Important electrical parameters are summarized for differential drive operation.

Nominal Differential Inductance:
$$L = \frac{\text{Im}(Z)}{\omega}$$

Quality Factor:
$$Q = \frac{|\text{Im}(Z)|}{|\text{Re}(Z)|}$$

Division Ratio:
$$r = \frac{V_{p3} - V_{p2}}{V_{p1} - V_{p2}}$$

With $Z = z_{11} + z_{22} - (z_{12} + z_{21})$ and $\omega = 2\pi f$ (f: frequency)

5.2.1 Main Parameters of Differential Inductors

Inductor	Size [µm²]	Inductance [nH]	Qmax
DI15PT	186x186	1.5	14.5@13GHz
DI20PT	216x216	2.0	14@10GHz
DI25PT	252x252	2.5	14@8GHz
DI30PT	294x294	3.0	14@6GHz
DI35PT	342x342	3.5	14@5,3GHz
DI40PT	236x236	4.0	10@4,8GHz
DI45PT	286x286	4.5	10@3,8GHz
DI50PT	324x324	5.0	11@3,5GHz
DI55PT	354x354	5.5	11@3,2GHz
DI60PT	392x392	6.0	10@3GHz

Table 5.1 Size, Extracted nominal inductance and Qmax of differential inductors.

Note: Results are valid for thick metal module according to 1.2 (Process Family)

5.3 Characteristic Curves

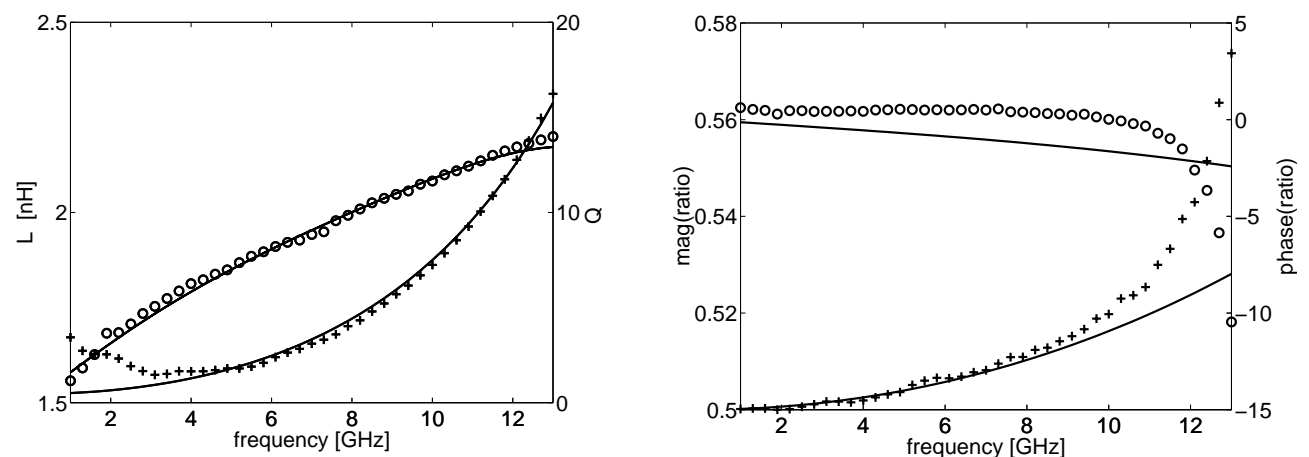


Fig. 5.2 Measured and simulated (-) differential inductance (+) and quality factor (o) of spiral DI15PT as a function of frequency. The magnitude (+) and phase (o) of the division ratio is shown on the right.

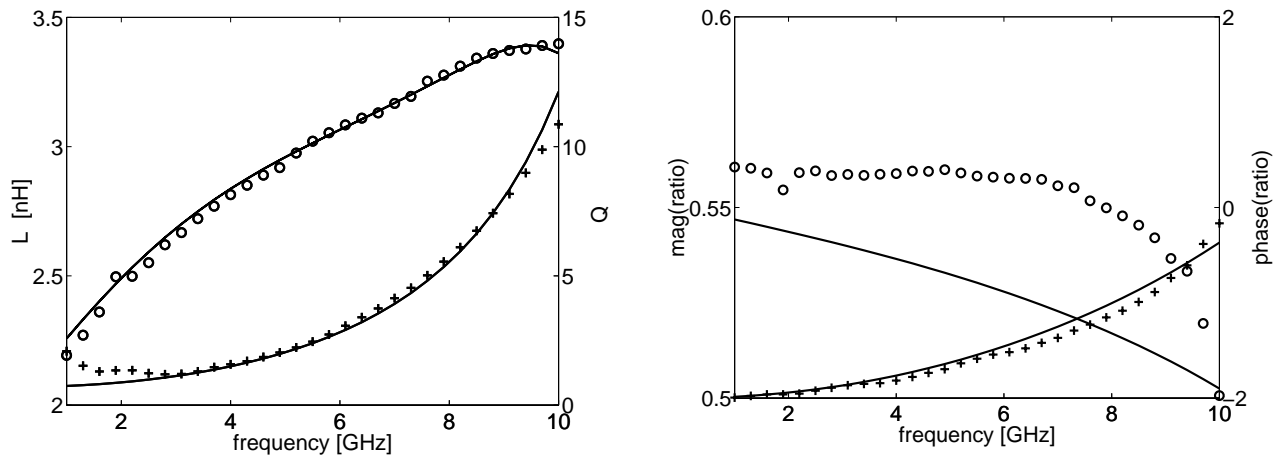


Fig. 5.3 Measured and simulated (-) differential inductance (+) and quality factor (o) of spiral DI20PT as a function of frequency. The magnitude (+) and phase (o) of the division ratio is shown on the right.

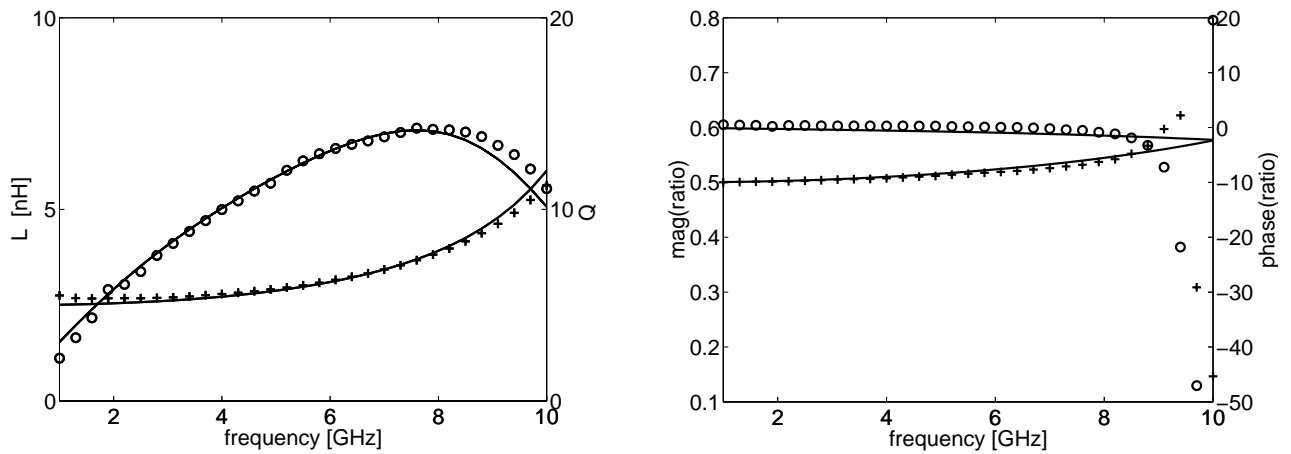


Fig. 5.4 Measured and simulated (-) differential inductance (+) and quality factor (o) of spiral DI25PT as a function of frequency. The magnitude (+) and phase (o) of the division ratio is shown on the right.

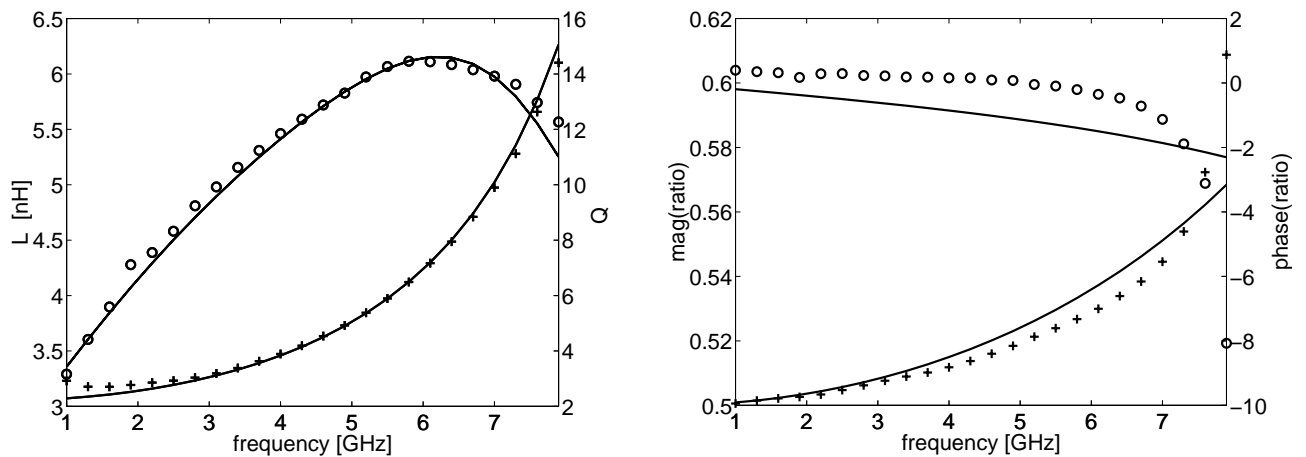


Fig. 5.5 Measured and simulated (-) differential inductance (+) and quality factor (o) of spiral DI30PT as a function of frequency. The magnitude (+) and phase (o) of the division ratio is shown on the right.

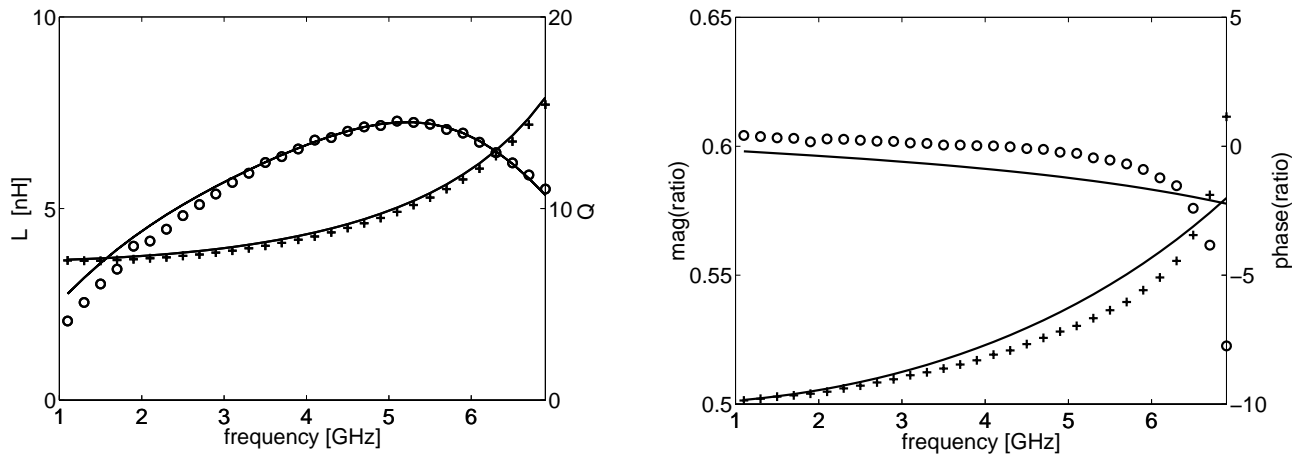


Fig. 5.6 Measured and simulated (-) differential inductance (+) and quality factor (o) of spiral DI35PT as a function of frequency. The magnitude (+) and phase (o) of the division ratio is shown on the right.

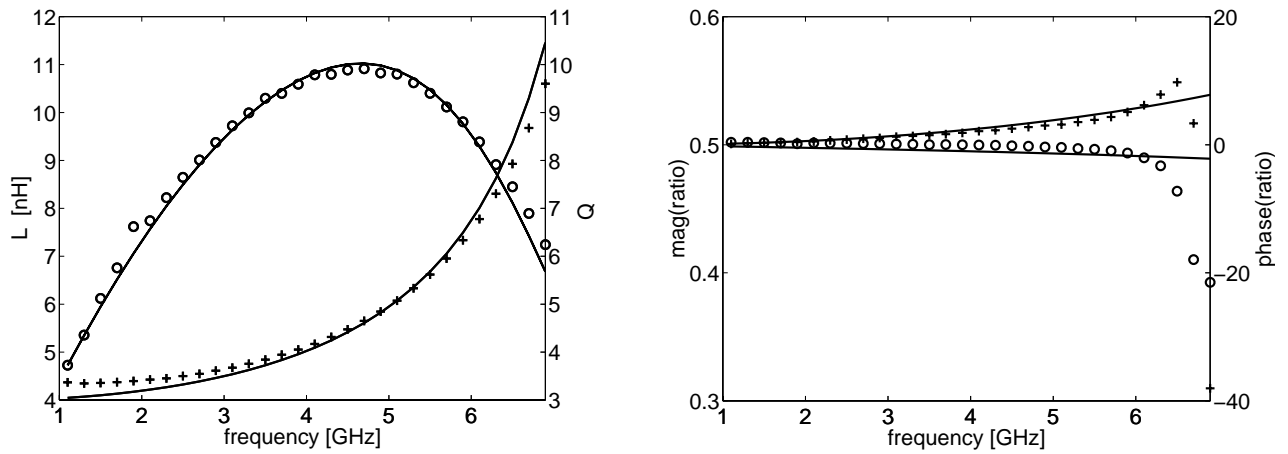


Fig. 5.7 Measured and simulated (-) differential inductance (+) and quality factor (o) of spiral DI40PT as a function of frequency. The magnitude (+) and phase (o) of the division ratio is shown on the right.

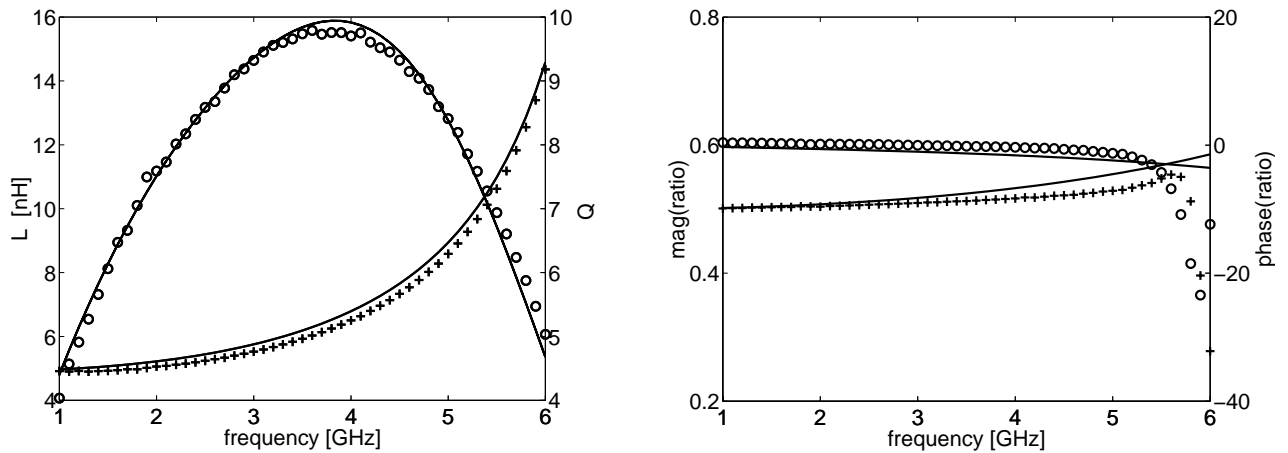


Fig. 5.8 Measured and simulated (-) differential inductance (+) and quality factor (o) of spiral DI45PT as a function of frequency. The magnitude (+) and phase (o) of the division ratio is shown on the right.

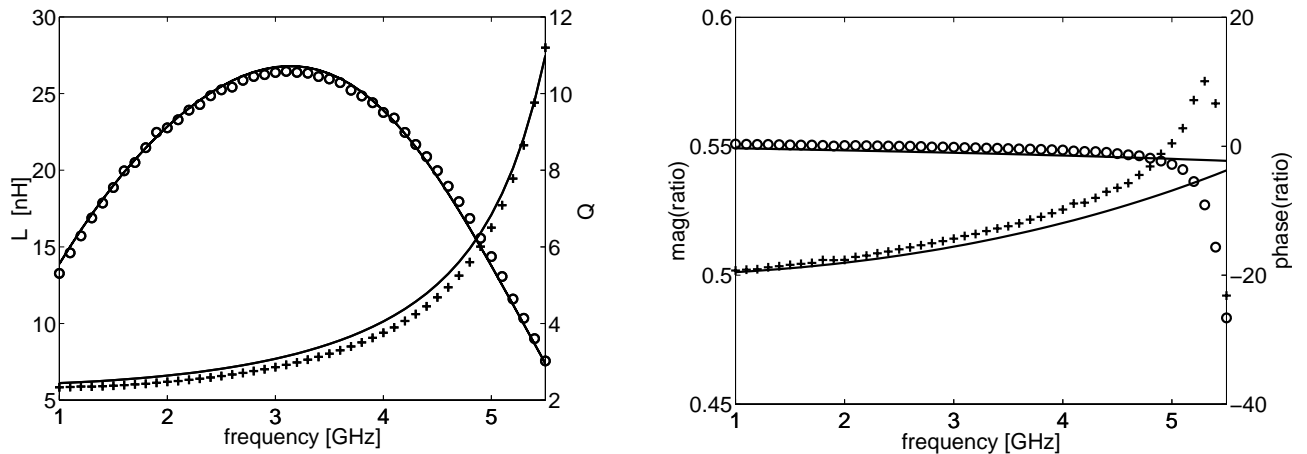


Fig. 5.9 Measured and simulated (-) differential inductance (+) and quality factor (o) of spiral DI50PT as a function of frequency. The magnitude (+) and phase (o) of the division ratio is shown on the right.

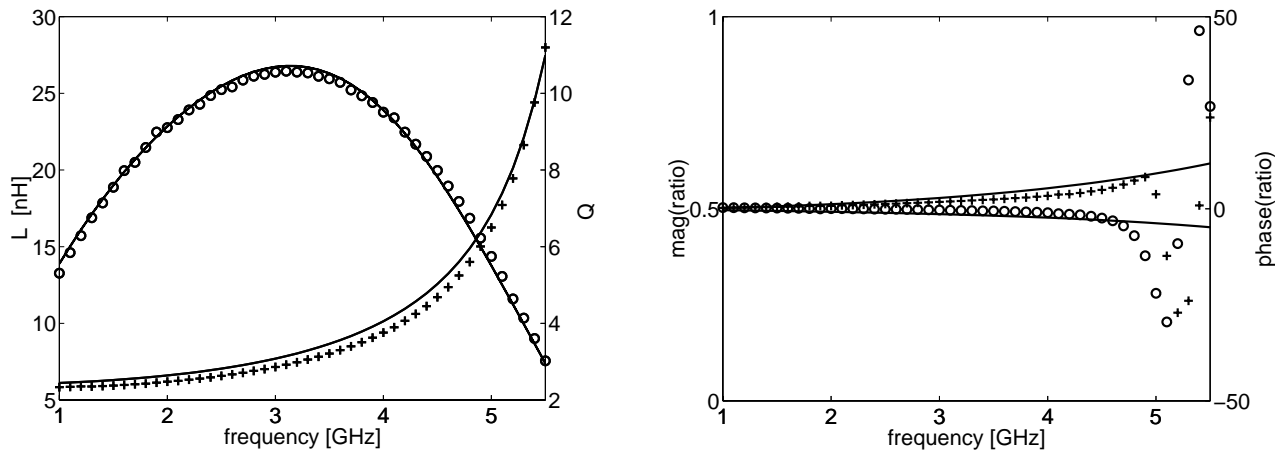


Fig. 5.10 Measured and simulated (-) differential inductance (+) and quality factor (o) of spiral DI55PT as a function of frequency. The magnitude (+) and phase (o) of the division ratio is shown on the right.

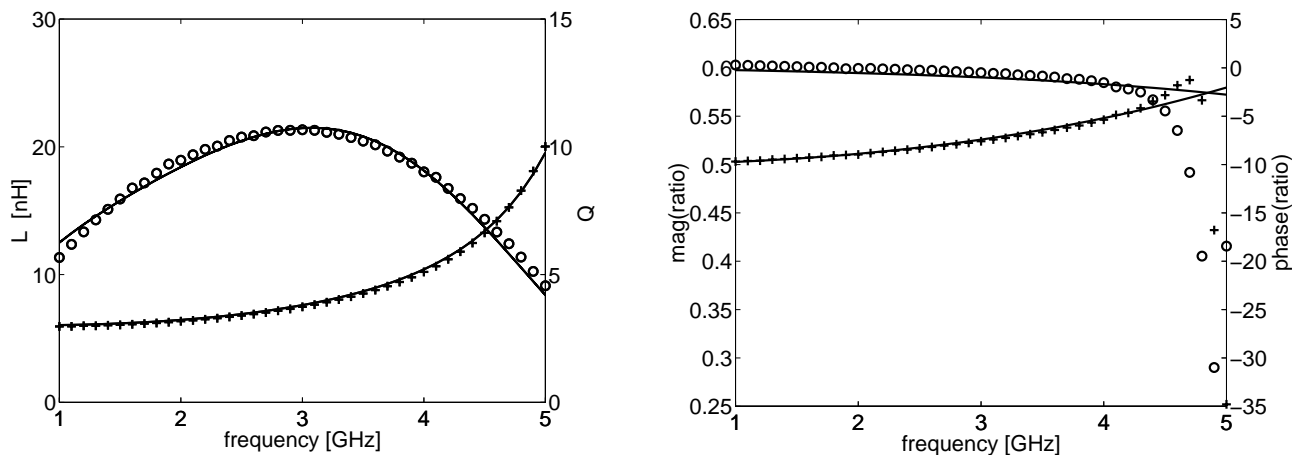


Fig. 5.11 Measured and simulated (-) differential inductance (+) and quality factor (o) of spiral DI60PT as a function of frequency. The magnitude (+) and phase (o) of the division ratio is shown on the right.

[2] Z. Huszka, "3-port characterization of differential inductors," IEEE BCTM, 14.3, pp. 269-272, 2004.

6 Poly1-Poly2 Capacitor (CPOLYRF)

The poly1-poly2 capacitor is built up of: poly2 (top-plate) - insulator (thin oxide) - poly1 (bottom-plate). Capacitors with values ranging from 0.1pF – 4pF and different W/L-ratios having the same area were measured. A scaleable model was extracted based on these measurements.

The model is valid in the following range:

Frequency range: up to 6 GHz

Capacitance range: 0.1 pF – 5pF

W/L: 1 – 2

Top plate contacts: placed over whole area

Bottom plate contacts: at least the opposite (longer) sides are contacted

WELL terminal (n-well) connected to the substrate or AC ground (e.g. Vcc)

6.1 Subcircuit Model

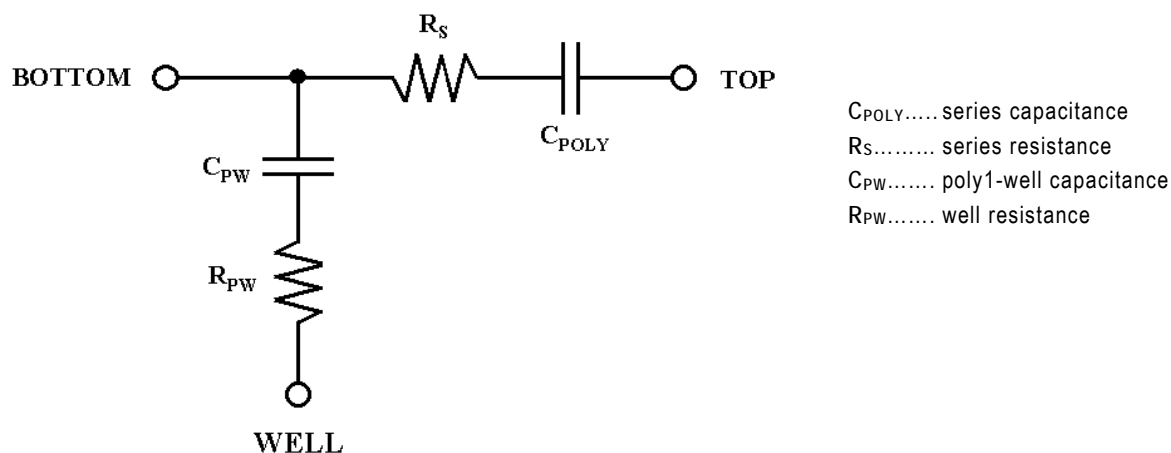


Fig.6.1 Subcircuit model of the poly1-poly2 capacitor.

6.2 Main Parameters

$$C_{poly} = -\frac{1}{\omega \text{Im}(Z)} \quad Q = \frac{|\text{Im}(Z)|}{|\text{Re}(Z)|}$$

With $Z=1/y_{22}$ and $\omega=2\pi f$ (f: frequency)

C [pF]	Q @ 2.4 GHz	Q @ 5 GHz
0.12	437	210
0.24	216	104
0.48	108	52
1.0	54	26
2.0	27	13
4.0	13.5	6.5

Table 6.1 Quality factors at different frequencies.

6.3 Characteristic Curves

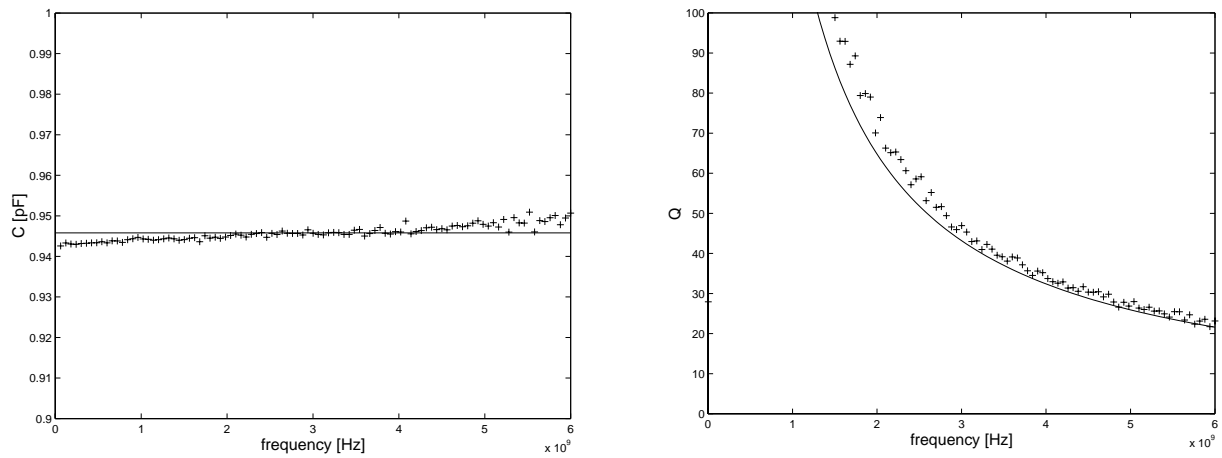


Fig. 6.2 Measured (+) and simulated (-) series capacitance and quality factor as a function of frequency ($W=33.9 \mu\text{m}$, $L=33.9 \mu\text{m}$).

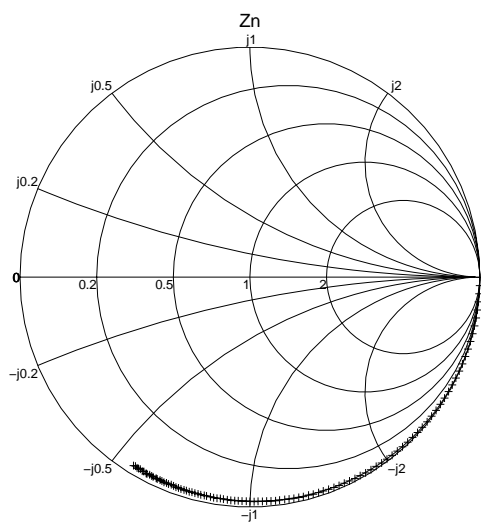


Fig. 6.3 Measured (+) and simulated (-) normalized impedance $Z_n=(Z-50)/(Z+50)$ ($W=33.9 \mu\text{m}$, $L=33.9 \mu\text{m}$).

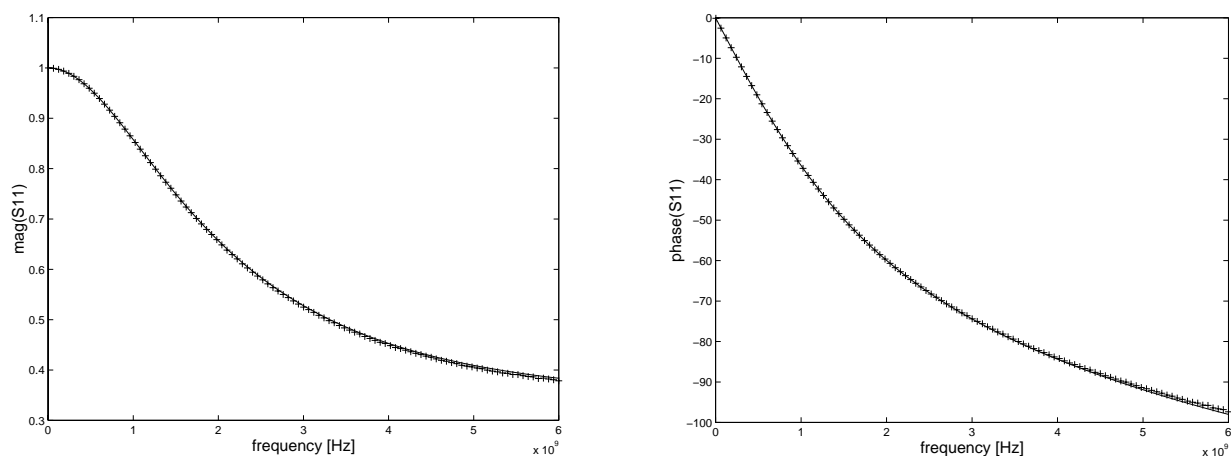


Fig. 6.4 Measured (x) and simulated (-) S_{11} (magnitude and phase), $W=33.9 \mu\text{m}$, $L=33.9 \mu\text{m}$.

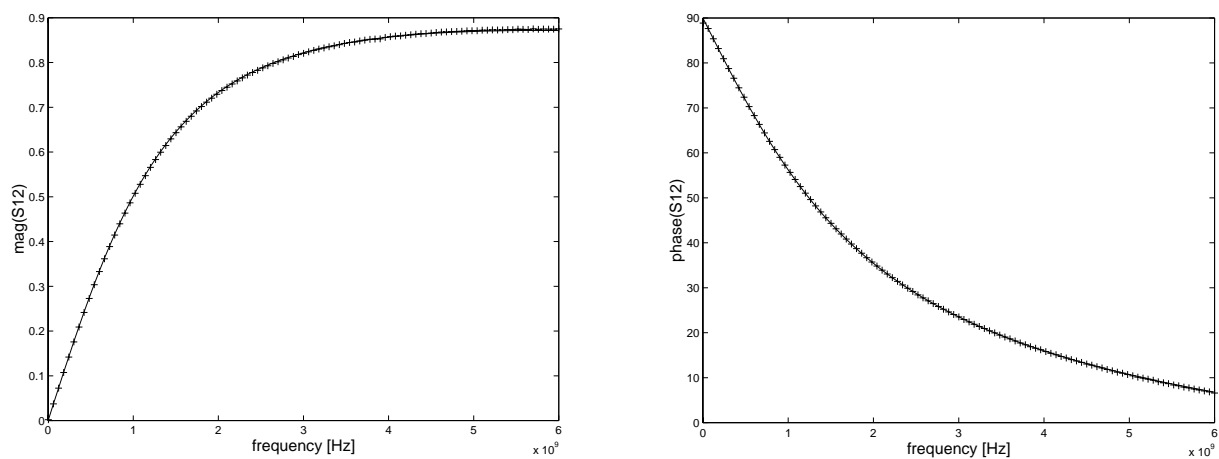


Fig. 6.5 Measured (x) and simulated (-) S_{12} (magnitude and phase), $W=33.9 \mu\text{m}$, $L=33.9 \mu\text{m}$.

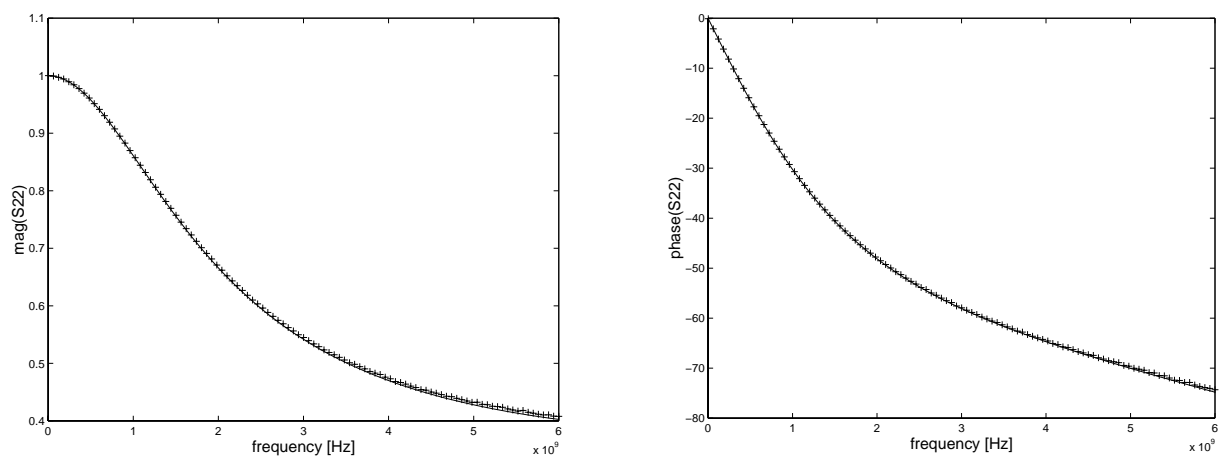


Fig. 6.6 Measured (x) and simulated (-) S_{22} (magnitude and phase), $W=33.9 \mu\text{m}$, $L=33.9 \mu\text{m}$.

7 Metal-Metal Capacitor (CMIM)

The metal-metal capacitor is built up of: METALC (top-plate) – insulator (silicon nitride) – METAL2 (bottom plate). Capacitors with values ranging from 0.1 pF – 1 pF were measured. Based on theoretical calculations the series resistance lies in the order of 0.1 Ω resulting in quality factors significantly exceeding 100. A state of the art measurement system is not capable of resolving such low resistances. The contacting metal path should have a width of at least 2 μm in order to preserve the high quality of the device.

The model is valid in the following range:

Frequency range: up to 6 GHz

Capacitance range: 0.1 pF – 1 pF

WELL terminal (n-well) connected to the substrate or AC ground (e.g. Vcc)

7.1 Subcircuit Model

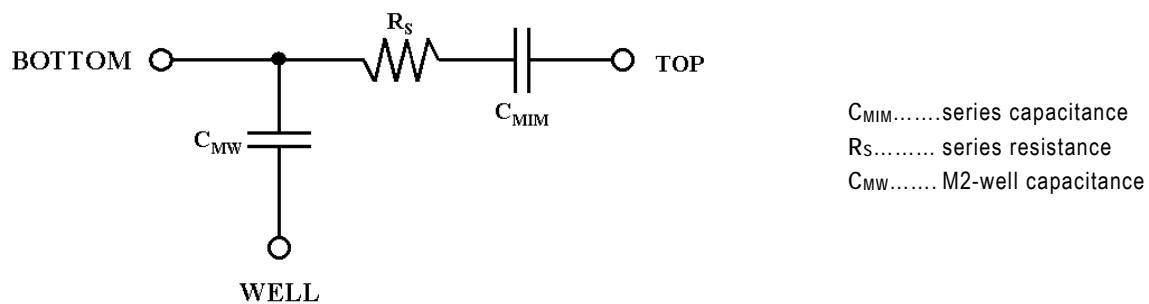


Fig.7.1 Subcircuit model of the MIM capacitor.

Note: The major Q limiting factor is the top plate contact resistance. R_s is calculated based on the VIA2 contact resistance.

7.2 Characteristic Curves

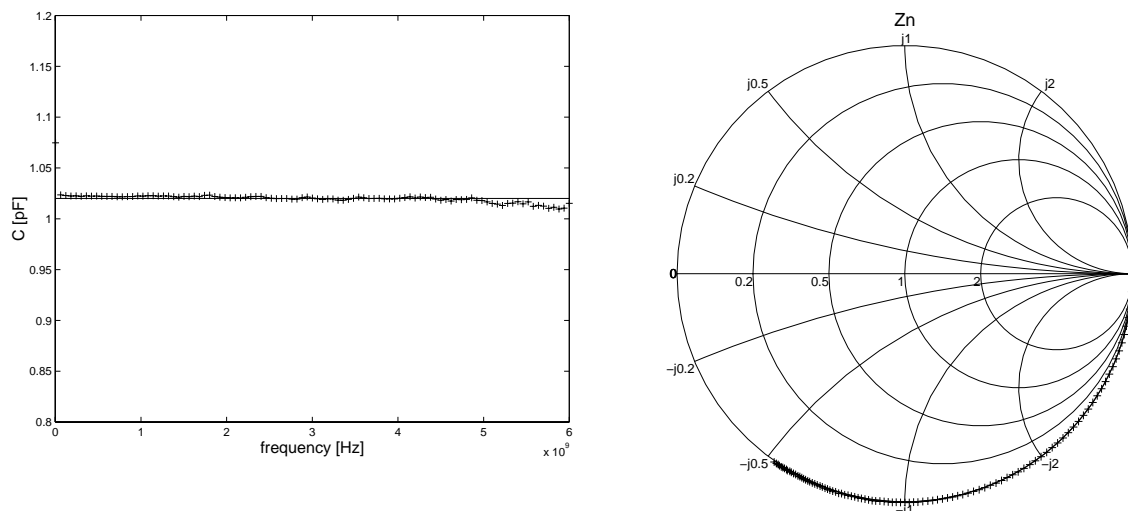


Fig. 7.2 Measured (x) and simulated (-) series capacitance and normalized impedance $Z_n = (Z-50)/(Z+50)$ ($W=28.85 \mu\text{m}$, $L=28.85 \mu\text{m}$).

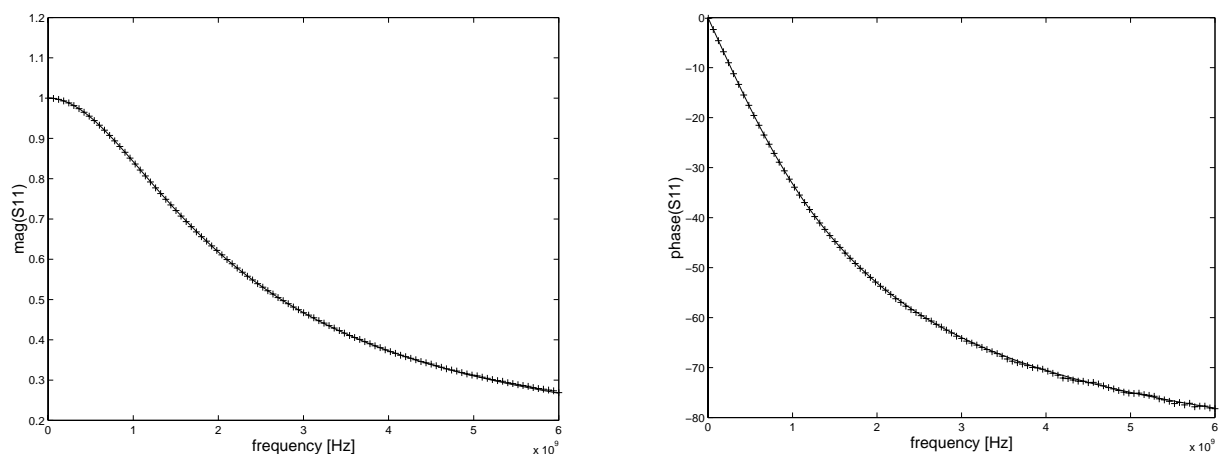


Fig. 7.3 Measured (x) and simulated (-) S_{11} (magnitude and phase), $W=28.85 \mu\text{m}$, $L=28.85 \mu\text{m}$.

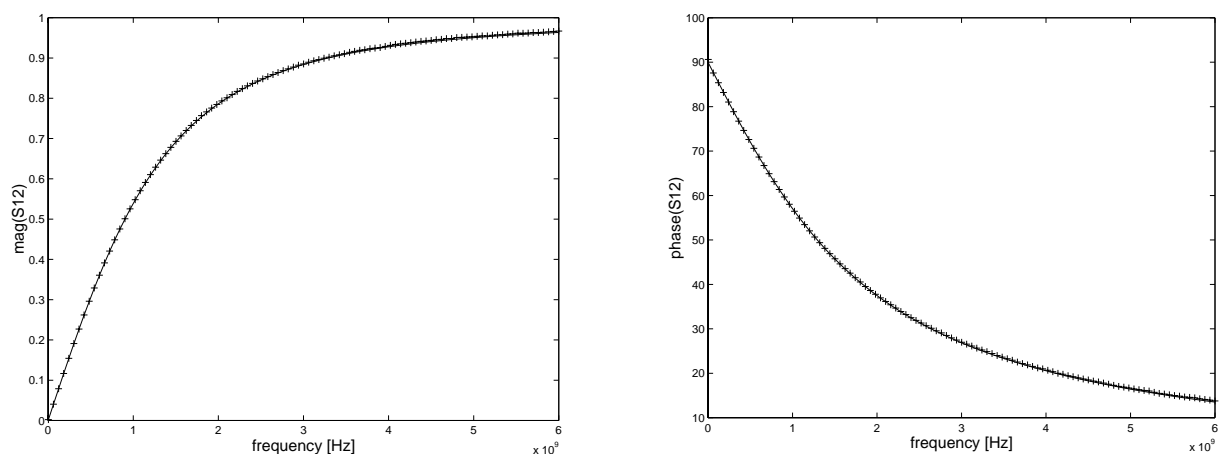


Fig. 7.4 Measured (x) and simulated (-) S_{12} (magnitude and phase), $W=28.85 \mu\text{m}$, $L=28.85 \mu\text{m}$.

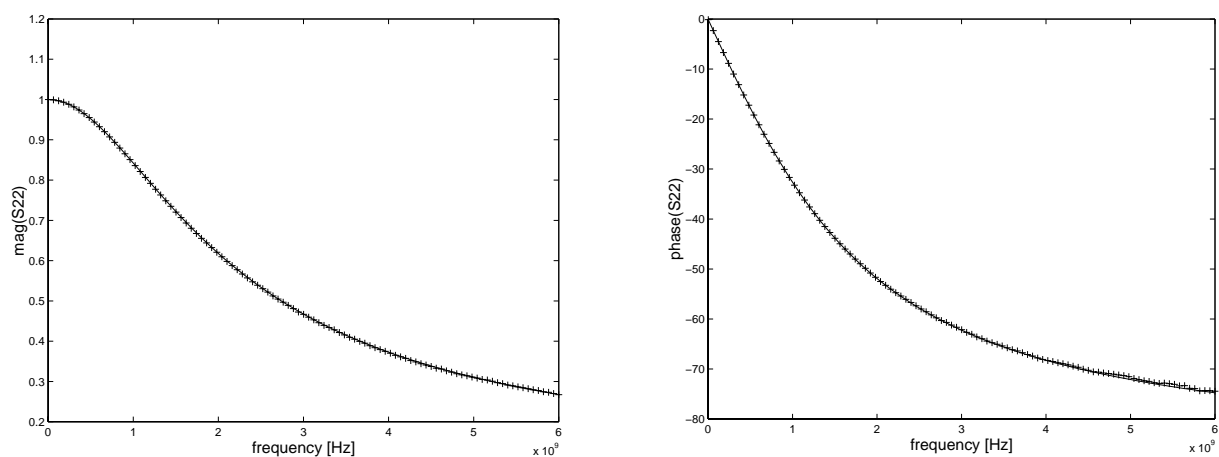


Fig. 7.5 Measured (x) and simulated (-) S_{22} (magnitude and phase), $W=28.85 \mu\text{m}$, $L=28.85 \mu\text{m}$.

8 Poly Resistors (RPOLY2RF, RPOLYHRF)

Rpoly2 and Rpolyh (high resistive poly) resistors having a width of 1, 2 and 3 μm and different L/W ratios were measured. The performances of straight line, meander type and segmented type of structures have also been investigated. A scaleable model was extracted.

The model is valid in the following range:

Frequency range: up to 6 GHz

W (drawn): 1 μm – 3 μm

Maximum length of Rpoly2: 90 μm

Maximum length of Rpolyh: 30 μm

WELL terminal (n-well) connected to the substrate or AC ground (e.g. Vcc)

8.1 Subcircuit Model

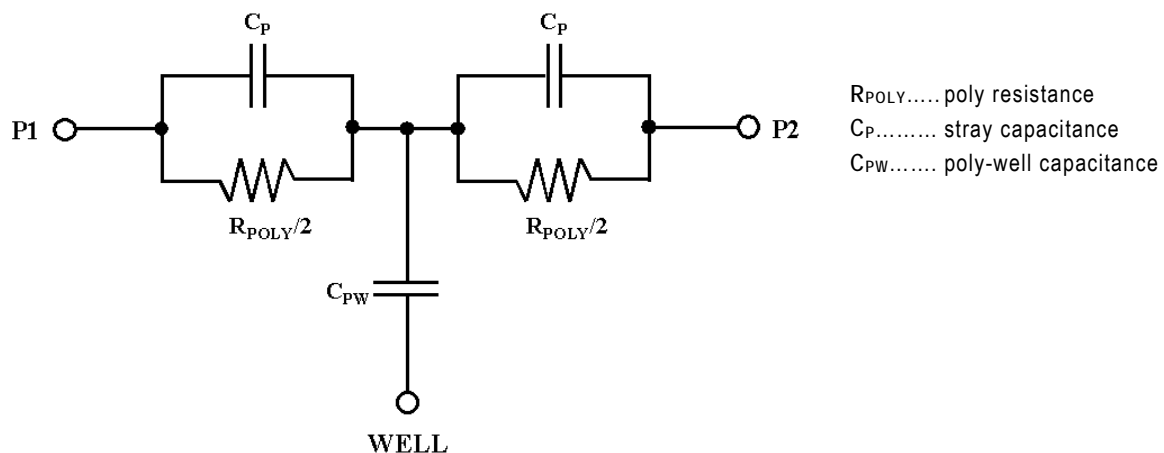


Fig.8.1 Subcircuit model of poly resistors.

8.2 Main Parameters

$$\text{P1-P2 drive: } R_{P1P2} = \text{Re}(Z_{P1P2}) \quad Q_{P1P2} = \frac{|\text{Re}(Z_{P1P2})|}{|\text{Im}(Z_{P1P2})|}$$

$$\text{P1 drive: } R_{P1} = \text{Re}(Z_{P1}) \quad Q_{P1} = \frac{|\text{Re}(Z_{P1})|}{|\text{Im}(Z_{P1})|}$$

With $Z_{P1}=1/y_{11}$, $Z_{P1P2}=Z_{11}+Z_{22}-(Z_{12}+Z_{21})$ and $\omega=2\pi f$ (f: frequency)

Note: In the case of a resistor Q is the ratio of the real to the imaginary part of the impedance. The loss of resistance is the signal absorbed by the parallel reactance.

8.3 Characteristic Curves

8.3.1 Characteristic Curves of Rpoly2 Resistors

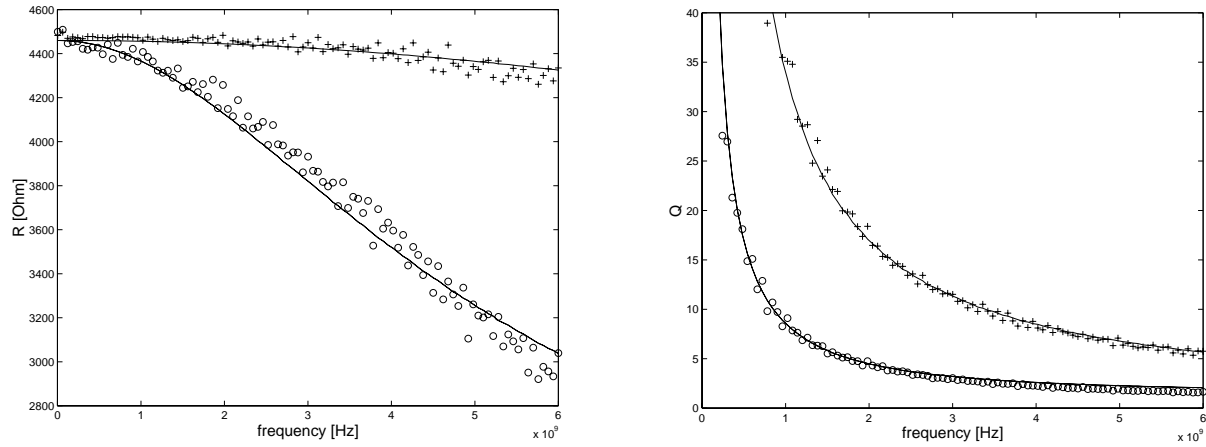


Fig. 8.2 Measured and simulated (-) P1-P2 (+) and P1 (o) drive resistance and Q of Rpoly2 ($L=60\ \mu\text{m}$, $W=1\ \mu\text{m}$) as a function of frequency.

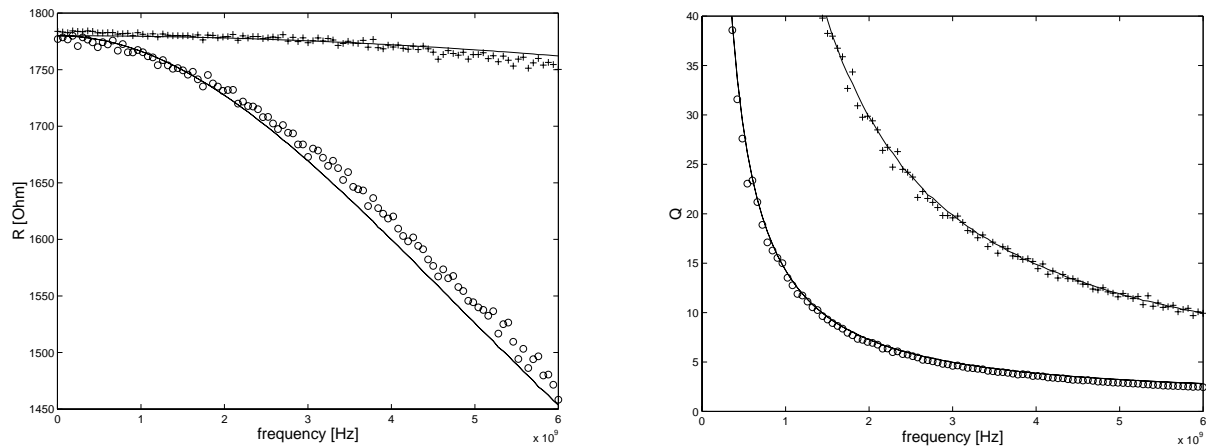


Fig. 8.3 Measured and simulated (-) P1-P2 (+) and P1 (o) drive resistance and Q of Rpoly2 ($L=60\ \mu\text{m}$, $W=2\ \mu\text{m}$) as a function of frequency.

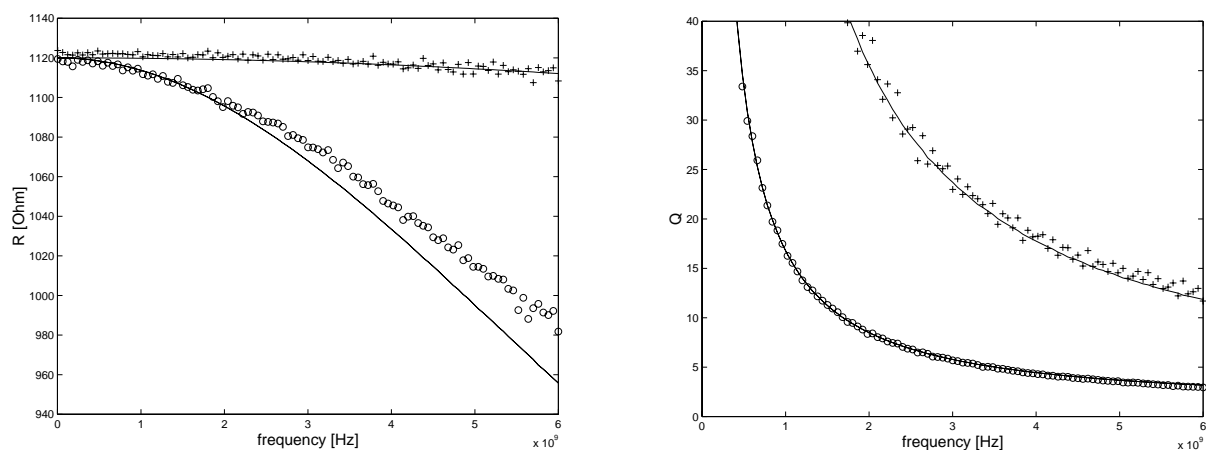


Fig. 8.4 Measured and simulated (-) P1-P2 (+) and P1 (o) drive resistance and Q of Rpoly2 ($L=60\ \mu\text{m}$, $W=3\ \mu\text{m}$) as a function of frequency.

8.3.2 Characteristic Curves of Rolyh Resistors

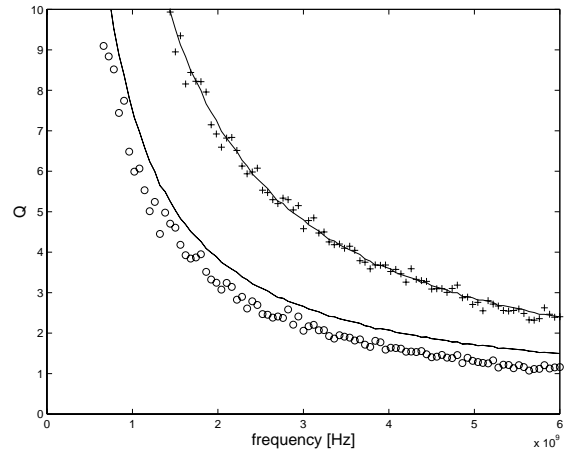
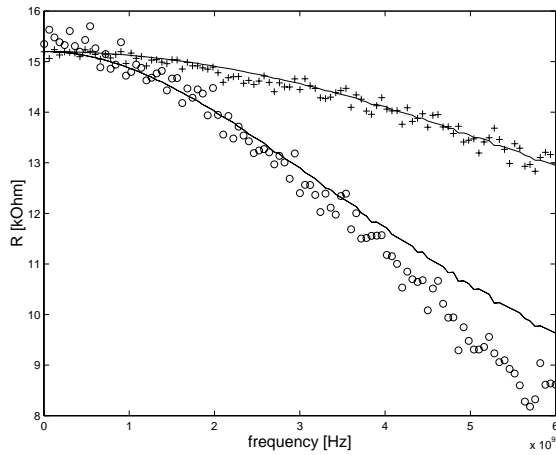


Fig. 8.5 Measured and simulated (-) P1-P2 (+) and P1 (o) drive resistance and Q of Rpolyh ($L=10\ \mu\text{m}$, $W=1\ \mu\text{m}$) as a function of frequency.

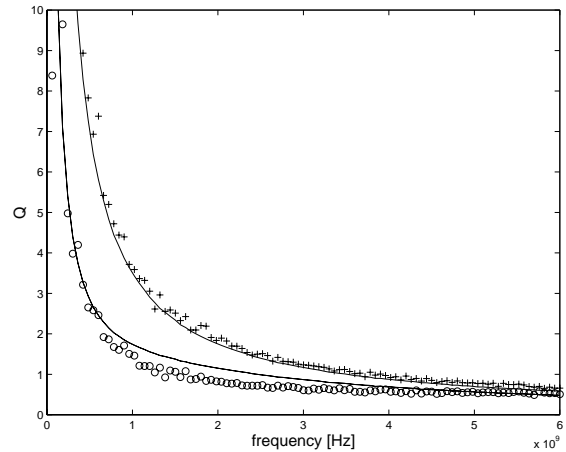
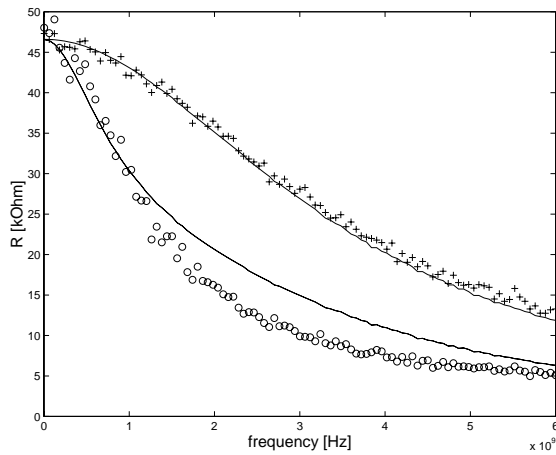


Fig. 8.6 Measured and simulated (-) P1-P2 (+) and P1 (o) drive resistance and Q of Rpolyh ($L=30\ \mu\text{m}$, $W=1\ \mu\text{m}$) as a function of frequency.

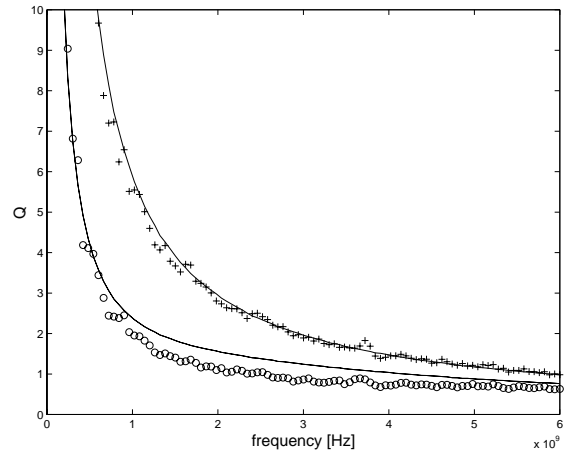
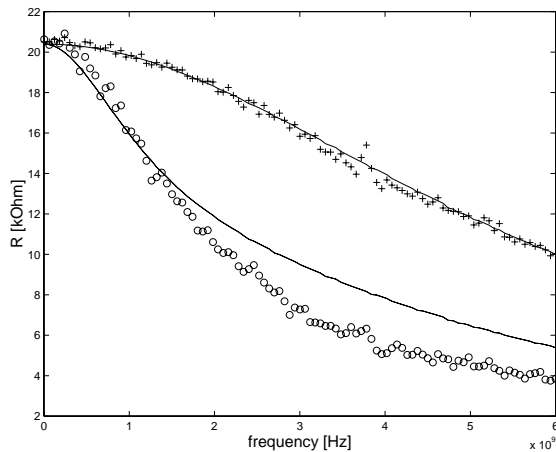


Fig. 8.7 Measured and simulated (-) P1-P2 (+) and P1 (o) drive resistance and Q of Rpolyh ($L=30\ \mu\text{m}$, $W=2\ \mu\text{m}$) as a function of frequency.

9 Summary of RF SPICE Models

Device	Device Name	Model Name	Model Rev.
NMOS transistor	NMOSRF	modnrf	3.0
PMOS transistor	PMOSRF	modprf	3.0
MOS varactor	CVAR	cvar	3.0
Inductors	STXXXAYYYB	stxxxayyyb	3.0
Differential Inductors	DIXXPT	dixxpt	1.0
Poly1-Poly2 capacitor	CPOLYRF	cpolyrf	4.0
Metal-metal capacitor	CMIMRF	cmimrf	1.0
Poly2 resistor	RPOLY2RF	rpoly2rf	4.0
Polyh resistor	RPOLYHRF	rpolyhrf	1.0

The indicated model revision relates to the actual implementation of the simulator model. Changes and updates of the simulator model lead to an update of the revision number and are documented within the actual model files and on the technical webserver (see below).

10 Simulator Models and Design Kit Integration

RF models are supported for the following simulators and integrated within the following CAD environments of the austriamicrosystems HIT-Kit:

Simulator	Simulator Version	CAD Integration
Spectre	5.1.41	Cadence IC5.1.41
ADSSim	v2004a	Agilent ADS v2004
ELDO	6.5.2	Anacad v2005.2

The mos varactor model is provided for the following circuit simulators and compact models:

Simulator	BSIM3v3 Version
Spectre	BSIM3V3.2
ELDO	
Hspice	
Smartspice	
Saber	
Smash	
ADSSim	

Due to continuous model improvement the device models and parameters are subject to regular updates documented on the ASIC server of austriamicrosystems AG. Actual simulator models can be downloaded from the download area.

Updates of model revision/ netlist format/ simulation parameters:

<http://asic.austriamicrosystems.com>

11 Note on S-parameter measurements

Linear or nonlinear networks operating with small-signals (sufficiently small to cause the networks to respond in a linear manner) can be completely characterized by parameters measured at the network terminals (ports) without regard to the contents of the network. Scattering parameters or commonly referred to as s-parameters have the advantage that they can be measured easier at high frequencies using a vector network analyzer (VNA) than other kinds of parameters, which makes them well suited for describing passive and active devices. RF measurements are always influenced by parasitic components (e.g. pads). Advanced dummy structures and de-embedding techniques eliminate their effect on the measurements. The s-parameter measurements have been performed in two-port configuration. S-parameter plots are shown in each section to demonstrate the quality of the models.

12 Support

For questions on process parameters please refer to:

austriamicrosystems AG
A 8141 Schloss Premstätten, Austria
T. +43 (0) 3136 500 0
F. +43 (0) 3136 525 01
E-mail: tips@austriamicrosystems.com
Technical Webserver: <http://asic.austriamicrosystems.com>
Homepage: <http://www.austriamicrosystems.com>

13 Copyright

Copyright © 2005 austriamicrosystems AG. Trademarks registered ®. All rights reserved. The material herein may not be reproduced, adapted, merged, translated, stored, or used without the prior written consent of the copyright owner. To the best of its knowledge, austriamicrosystems asserts that the information contained in this publication is accurate and correct.